HAW HAMBURG

Bachelor Thesis

Christian Rösing

Design of a Hydrogen Fuel Cell Powered Long-Endurance Drone for Wildfire Detection

Fakultät Technik und Informatik

Department Fahrzeugtechnik und Flugzeugbau

Faculty of Engineering and Computer Science

Department of Automotive and Aeronautical Engineering

Christian Rösing

Design of a Hydrogen Fuel Cell Powered Long-Endurance Drone for Wildfire Detection

Bachelor thesis submitted as part of the bachelor examination.

Degree program: Aeronautical Engineering
Department of Automotive and Aeronautical Engineering
Faculty of Engineering and Computer Science
Hamburg University of Applied Sciences

First examiner: Prof. Dr.-Ing. Dieter Scholz, MSME
Second examiner, supervisor: Kay Wackwitz, Dipl-Ing. (FH)

Submitted: 2023-12-16

DOI:
https://doi.org/10.5281/zenodo.15619985

URN:
https://nbn-resolving.org/urn:nbn:de:gbv:18302-aero2023-12-16.011
Associated URLs:
https://nbn-resolving.org/html/urn:nbn:de:gbv:18302-aero2023-12-16.011

Any further request may be directed to:
Prof. Dr.-Ing. Dieter Scholz, MSME
E-Mail see: http://www.ProfScholz.de

This work is part of:
Digital Library - Projects & Theses - Prof. Dr. Scholz
http://library.ProfScholz.de

Published by
Aircraft Design and Systems Group (AERO)
Department of Automotive and Aeronautical Engineering
Hamburg University of Applied Science

This report is deposited and archived:
- Deutsche Nationalbiliothek (https://www.dnb.de)
- ZENODO (https://zenodo.org/communities/digitallibrary)
- Internet Archive (https://archive.org)
  Item: https://archive.org/details/TextRoesingBachelor.pdf

This report has associated published data in Harvard Dataverse:
https://doi.org/10.7910/DVN/JKKX2M

Name of student
Christian Rösing

Title of the report
Design of a Hydrogen Fuel Cell Powered Long-Endurance Drone for Wildfire Detection

Keywords (LCSH)
Aeronautics, Drone aircraft--Design and construction, Hydrogen as fuel, Fuel cells, Propellers, Aerial, Aerodynamics, Lift (Aerodynamics), Drag (Aerodynamics), Airframes, Airfoils, Airplanes--Fuselage, [Aircraft design, Empennage]

Abstract

Purpose – In this bachelor thesis, a drone is developed that will be used for early wildfire detection. The drone should also be able to be used by authorities to detect oil spills or to provide live images in the event of disasters and large-scale emergency operations. In order to keep noise and environmental pollution in the area of operation as low as possible, the drone is to be powered by hydrogen with fuel cells.
Methodology – The calculations are based on scripts by Professor Scholz on aircraft design and Professor Sadraey on the design of unmanned aerial systems. Microsoft Excel was used to calculate the matching charts. The requirements for such a drone have been discussed with potential customers and authorities, as well as aid organizations that are already using drones.
Findings – The results from the draft do not meet all the previously established requirements. The flight time and also the range fall far short of expectations. During the design, many assumptions had to be made that have not yet been confirmed by empirical values.
Practical implications – The results achieved in the design make it clear that the use of hydrogen poses many challenges. It turns out that hydrogen propulsion is currently associated with high weight and short ranges and that empirical values urgently need to be gained in order to optimize the design of hydrogen-powered aircraft.
Social implications – The draft shows a possibility that allows the use of environmentally friendly technology to protect the population. In addition, the challenges faced for the use of this technology are shown.
Originality/value – This is the first time that a design has been developed with this detail using the methods for conventional transport aircraft in conjunction with the methods for unmanned aerial vehicles for a hydrogen-powered drone. The challenges and limitations of a hydrogen-powered aircraft are demonstrated for the first time.

Name des Studierenden
Christian Rösing

Thema der Bachelorarbeit
Design of a Hydrogen Fuel Cell Powered Long-Endurance Drone for Wildfire Detection

Stichworte (GND)
Luftfahrt, Drohne, Entwurf, Wasserstoff, Propellerflugzeug, Brennstoffzelle, Aerodynamik, Auftrieb, Luftwiderstand, Tragflügel, Leitwerk <Flugzeug>, Rumpfwerk, [Flugzeugentwurf]

Kurzreferat

Zweck – In dieser Bachelorarbeit wird eine Drohne entwickelt, die zur Waldbrandfrüherkennung eingesetzt werden soll. Die Drohne soll zusätzlich auch von Behörden eingesetzt werden können, um Ölteppiche zu erkennen, oder bei Katastrophen und Großeinsätzen Livebilder liefern zu können. Um die Lärm- und Umweltbelastung im Einsatzgebiet möglichst gering zu halten, soll die Drohne einen Wasserstoffantrieb mit Brennstoffzellen haben.
Methodik – Die Berechnungen erfolgen auf Grundlage von Skripten von Professor Scholz zum Flugzeugentwurf und Professor Sadraey zum Entwurf von unbemannten Luftfahrzeugen. Zur Berechnung der Entwurfsdiagramme wurde Microsoft Excel verwendet. Die Anforderungen an eine solche Drohne wurden mit möglichen Kunden und Behörden sowie Hilfsorganisationen, die bereits Drohnen einsetzen, erörtert.
Ergebnisse – Die Ergebnisse aus dem Entwurf erfüllen nicht alle zuvor festgelegten Anforderungen. Die Flugzeit und auch die Reichweite bleiben weit hinter den Erwartungen zurück. Während des Entwurfs mussten viele Annahmen getroffen werden, die durch Erfahrungswerte bisher nicht bestätigt werden können.
Bedeutung für die Praxis – Durch die erzielten Ergebnisse im Entwurf wird deutlich, dass der Einsatz von Wasserstoff viele Herausforderungen mit sich bringt. Es zeigt sich, dass zum jetzigen Zeitpunkt ein Wasserstoffantrieb mit hohem Gewicht und geringen Reichweiten verbunden ist und dringend Erfahrungswerte erlangt werden müssen, um den Entwurf von wasserstoffangetriebenen Flugzeugen zu optimieren.
Soziale Bedeutung – Der Entwurf zeigt eine Möglichkeit auf, die den Einsatz von umweltverträglicher Technik zum Schutz der Bevölkerung zulässt. Zusätzlich wird aufgezeigt mit welchen Herausforderungen für den Einsatz dieser Technik zu kämpfen ist.
Originalität / Wert – Die Ausarbeitung eines Entwurfs mit den Methoden für konventionelle Transportflugzeuge in Verbindung mit den Methoden für unbemannte Luftfahrzeuge für eine Drohne mit Wasserstoffantrieb findet in dieser Ausführlichkeit das erste Mal statt. Die Herausforderungen und Grenzen eines Luftfahrzeugs mit Wasserstoffantrieb werden erstmals aufgezeigt.

HAW HAMBURG

DEPARTMENT OF AUTOMOTIVE AND AERONAUTICAL ENGINEERING

Design of a Hydrogen Fuel Cell Powered Long-Endurance Drone for Wildfire Detection

Task for a Bachelor Thesis

Background

Due to fast-proceeding climate change and resulting droughts also in Europe, more and more woodland is under threat of wildfires. An early detection of wildfires is crucial to suppress fires before they grow too big. As such, the costs and risks of a firefighting campaign can be kept down. Until now, regular manned small fixed-wing aircraft with gasoline engines are used to patrol and overfly threatened forest lands at high financial and environmental costs. Other methods in use are manned observation outposts or tower-attached cameras. But all these methods cannot provide a gapless monitoring of wide areas. On the contrary, an unmanned fleet of hydrogen powered aerial systems could have the potential to close the gaps. It could offer a 24-hour observation service, could be more flexible and could have lower climate impact and less noise pollution compared to conventional wildfire detection.

Task

Task of this thesis is to apply the method of preliminary sizing to design a hydrogen fuel cell powered drone for early wildfire detection. The drone should have a flight time as long as possible to keep operation costs low and should carry about 10 kg of payload in the form of cameras and sensors. Following subtasks have to be considered:

- Request system requirements from possible clients.
- Define requirements of the flying platform and mission.
- Evaluate design drafts regarding the defined requirements.
- Do a trade-off study of existing drone models with similar applications and specifications.
- Define an aircraft configuration and propulsion system.
- Calculate take-off mass, fuel mass, operating empty mass, wing area, and power of the propulsion system.
- Calculate the mass distribution and ascertain the position of the center of gravity.
- Calculate wing dimensions (aspect ratio, wing position, …).
- Determine an empennage layout, calculate the dimensions and position.

The report has to be written in English based on German or international standards on report writing.

Table of Contents

List of Figures

List of Tables

List of Symbols

A / AR	Aspect ratio [-]
b	Wingspan [m]
C	Coefficient [-]
c	Chord length [m]
D	Drag [N]
E_D	Energy density $\left[\frac{\mathrm{Wh}}{\mathrm{kg}}\right]$
e	Oswald efficiency factor [-]
F	Force [N]
g	Gravitational constant $\left[\frac{\mathrm{m}}{\mathrm{s}^2}\right]$
h	Altitude [m]
K	Correction factor [-] / Induced drag factor [-]
K'	Empirical correction factor for nonlinear effects
L	Lift [N]
l	Lever [m]
M	Mach number [-] / Momentum [Nm]
m	Mass [kg]
N	Momentum [Nm]
n	Number [-]
P	Power [W]
R	Range [m]
ROC	Rate of climb $\left[\frac{\mathrm{m}}{\mathrm{s}}\right]$
S	Area [m^2]
s	Length [m]
T	Thrust [N]
t	Time [s]
u	Useful load [-]
V	Speed $\left[\frac{\mathrm{m}}{\mathrm{s}}\right]$
W	Weight [N]
x	x-Position [mm] / [m]
y	y-Position [mm] / [m]
z	z-Position [mm] / [m]

Greek Symbols

Δ	Difference [-]
δ_F	Deflection angle of the rudder [deg] / [rad]
η	Efficiency [-]
Λ / φ	Sweep angle [deg] / [rad]
λ	Taper ratio [-]
μ	Friction coefficient [-]
ρ	Air density $\left[\frac{\mathrm{kg}}{\mathrm{m}^3}\right]$
σ	Air density ratio [-]

Indices

0	Zero-lift / AMSL
25	25 %-position of chord length
AC	Aerodynamic center / Absolute ceiling
B	Battery
C	Cruise / Ceiling
CG	Center of gravity
CR	Cruise
D	Drag
E	Engine / Empty
F	Fuel
G	Ground
GW	Gross weight
H	Horizontal
L	Landing / Lift
LG	Landing gear
m	Mission
max	Maximum
MC	Minimum control
MTO	Maximum take-off
OE	Operating empty
P	Propeller
PL	Payload
R	Rotation
S	Stall
SL	Sea level
TO	Take-off
TOFL	Take-off field length
V	Vertical
W	Wing

List of Abbreviations

AC	Aerodynamic Center
AI	Artificial Intelligence
AMSL	Above Mean Sea Level
BBK	Bundesamt für Bevölkerungsschutz und Katastrophenhilfe (engl.: Federal Agency of Civil Protection and Disaster Relief)
BWB	Blended Wing Body
BUKEA	Behörde für Umwelt, Klima, Energie und Agrarwirtschaft (engl.: Administration of Environment, Climate, Energy and Agriculture)
CAD	Computer Aided Design
CG	Center of Gravity
DAA	Detect and Avoid
FOD	Foreign Object Debris / Foreign Object Damage
GPS	Global Positioning System
GW	Gross Weight
HALE	High Altitude Long Endurance Drone
HU	Institut für Hygiene und Umwelt (engl.: Institute of Hygiene and Environment) Hamburg
IR	Infrared
L/D	Lift-to-Drag Ratio
LiDAR	Light Detection and Ranging
MALE	Medium Altitude Long Endurance Drone
MTOW	Maximum Take-off Weight
N/A	Not Available / Not Applicable
RGB-camera	Optical camera for visible light
ROC	Rate of Climb
UAV	Unmanned Aerial Vehicle
VTOL	Vertical Take-off and Landing

Definitions

Configuration
The definition from the Merriam Webster Dictionary of the word *configuration*, among other things, is a "relative arrangement of parts or elements" (Merriam Webster 2023a).

Disaster
Due to a definition from the Encyclopedia Britannica, a *disaster* is "any natural or human-generated calamitous event that produces great loss of human life or destruction of the natural environment, private property, or public infrastructure" (Encyclopedia Britannica 2023a).

Empennage
The *empennage* is, as defined by the Collins Dictionary, "the tail assembly of an airplane, consisting of vertical and horizontal stabilizers, and including the fin, rudder, and elevators" (Collins Dictionary 2023c).

Environmental impact
The term *environmental impact* is defined by the Fundación MAPFRE as:

> *It is the effect of human activity on the environment in the form of creating environmental imbalance.*
>
> *Some of the most common environmental impacts are:*
> *• air pollution*
> *• water pollution (seas, rivers, groundwater)*
> *• soil pollution*
> *• waste production*
> *• noise pollution*
> *• damage to ecosystems and loss of biodiversity* (MAPFRE 2023)

Gas cylinder
The definition of a *gas cylinder* is, due to the Collins Dictionary, "a cylinder-shaped container in which gas is kept under pressure" (Collins Dictionary 2023d).

Greenhouse gases
The Encyclopedia Britannica defines *greenhouse gases* as follows:

> *... any gas that has the property of absorbing infrared radiation (net heat energy) emitted from Earth's surface and reradiating it back to Earth's surface, thus contributing to the greenhouse effect. Carbon dioxide, methane, and water vapour are the most important greenhouse gases. (To a lesser extent, surface-level ozone, nitrous oxides, and fluorinated gases also trap infrared radiation.) Greenhouse gases have a profound effect on the energy budget of the Earth system despite making up only a fraction of all atmospheric gases.* (Encyclopedia Britannica 2023b)

LiDAR-System

The National Oceanic and Atmospheric Administration describes a *LiDAR-System* as follows:

> *Lidar, which stands for Light Detection and Ranging, is a remote sensing method that uses light in the form of a pulsed laser to measure ranges (variable distances) to the Earth. These light pulses—combined with other data recorded by the airborne system — generate precise, three-dimensional information about the shape of the Earth and its surface characteristics.* (NOAA 2023)

Loiter

By the definition of the DBpedia Association, *loiter* "is the phase of flight consisting of flying over some small region" (DBpedia 2023).

Medium Altitude Long Endurance drone (MALE)

By the definition from Unmanned Systems Technology, *Medium Altitude Long Endurance drones* are drones that "fly at altitudes of 10,000 to 30,000 feet" and "their enhanced flight time allows them to cover long ranges, unlocking a variety of applications" (UST 2023).

Patrol

The Collins Dictionary defines the word *patrol*, among other things, as "to make a regular and repeated circuit of (an area, town, camp, etc.) in guarding or inspecting" (Collins Dictionary 2023e).

Payload

The word *payload* is defined by the Merriam Webster Dictionary, among other things, as "the load carried by an aircraft or spacecraft consisting of people or things (such as passengers or instruments) necessary to the purpose of the flight" (Merriam Webster 2023b).

Performance

By a definition of the Merriam Webster Dictionary, *performance* is "the manner in which a mechanism performs" (Merriam Webster 2023c).

Requirement

The word *requirement* is defined by the Cambridge Dictionary as "something that is needed or demanded" (Cambridge Dictionary 2023b).

Rotation

The word *rotation* is described in an article from Wikipedia as "the action of applying back pressure to a control device, such as a yoke, side-stick or centre stick, to lift the nose wheel off the ground during takeoff. The aircraft rotates around its lateral axis" (Wikipedia 2023).

Tailplane

The word *tailplane* is defined by the Merriam Webster Dictionary as “the horizontal tail surfaces of an airplane including the stabilizer and the elevator” (Merriam Webster 2023d). The term is used in this thesis in combination with the words *horizontal* and *vertical* and refers therefore to both, the horizontal and the vertical stabilizer.

1 Introduction

1.1 Motivation

Due to climate change and longer periods of droughts the occurrence of wildfires is increasing. The use of unmanned aerial systems instead of manned aircraft can lead to the observation of more threatened areas. Drones can be used more mobile, an artificial intelligent software can analyze the live footage to determine possible wildfires, and with software support several drones could be controlled by a single operator. With interchangeable payloads, in this case cameras and sensors, not only wildfires could be detected, but also oil spillage and missing persons, meteorological data could be collected, or live footage of disasters and incident scenes could be provided to the authorities.

The design process of drones is not widely published at the moment, even less information can be found about the design of hydrogen powered aircraft. This thesis will offer a design of a hydrogen powered drone with wildfire and emergency observation abilities and show the challenges and limits that come with this design.

1.2 Title Terminology

Design
The Cambridge Dictionary defines the word *design*, among other things, as “the art of making plans or drawings for something” (Cambridge Dictionary 2023a).

Hydrogen
Due to a definition of the Collins Dictionary, *hydrogen* is “a colorless, odorless, flammable gas that combines chemically with oxygen to form water: the lightest of the known elements” (Collins Dictionary 2023a).

Fuel Cell
A *fuel cell* is defined by the Fuel Cell & Hydrogen Energy Association as:

> *A fuel cell is a device that generates electricity through an electrochemical reaction, not combustion. In a fuel cell, hydrogen and oxygen are combined to generate electricity, heat, and water. Fuel cells are used today in a range of applications, from providing power to homes and businesses, keeping critical facilities like hospitals, grocery stores, and data centers up and running, and moving a variety of vehicles including cars, buses, trucks, forklifts, trains, and more.*
>
> *Fuel cell systems are a clean, efficient, reliable, and quiet source of power. Fuel cells do not need to be periodically recharged like batteries, but instead continue to produce electricity as long as a fuel source is provided.* (FCHEA 2023)

Powered

The word *powered* is an adjective which is defined by Collins Dictionary as "a machine or vehicle [...]" that is operated with "[..] a specified fuel or prime mover" (Collins Dictionary 2023b).

Long-Endurance Drone

Unmanned Systems Technology defines *Long-Endurance Drones* as:

> *Long endurance drones provide a flight time greater than that of typical quadcopters and small fixed-wing UAV (unmanned aerial vehicles), which typically can only stay in the air for times ranging from half an hour to a couple of hours. Their enhanced flight time allows them to cover long ranges, unlocking a variety of applications.* (UST 2023)

Wildfire

The word *wildfire* is defined by National Geographic as follows:

> *A wildfire is an uncontrolled fire that burns in the wildland vegetation, often in rural areas. Wildfires can burn in forests, grasslands, savannas, and other ecosystems, and have been doing so for hundreds of millions of years. They are not limited to a particular continent or environment.* (National Geographic 2023)

Detection

The Britannica Dictionary defines the word *detection* as "the act or process of discovering, finding, or noticing something" (Britannica Dictionary 2023).

1.3 Objectives

This thesis will mainly provide a design for a drone used for long term observation of fire endangered areas. Due to lack of literature about the design of drones, this thesis also will provide a proof, that the methods of aircraft design used to this date can also be applied for drone design. In the end a design for a drone will be defined that can be used to provide a 24/7 service for wildfire detection. The usage of other emergency agencies, departments, and institutions as well as commercial interested parties can also be considered for times in which the drones are not in use for wildfire observation.

1.4 Literature Review

This constructional design thesis is mainly based on publications of Scholz (2015), a script written by Sadraey (2020) is used as an addition where the equations by Scholz are not useful. Besides Sadraey (2020) there were no further sources found which describe the design of drones with usable equations.

The lecture notes of Scholz about aircraft design sum up the design process as a short course and depict a detailed guideline with all needed sequences and equations for preliminary sizing and conceptual design of conventional aircraft of the transport category in 14 chapters. Although the lecture notes by Scholz are about aircraft of the transport category, the most important equations and variables can be used in this thesis and the described design steps will be followed where they are applicable for the design of a drone.

Scholz and the students supervised by Scholz use statistically determined factors for performance calculations. A statistical analysis to obtain those factors for drones was not possible, because the drone sector is surely a growing sector of aeronautics, but still quite small and appropriate information about similar designed drones were not available. To make those performance calculations the publication of Sadraey was used.

Sadraey provides in his publication a guideline for the design of unmanned aerial systems (UAS) of different types, like rotorcraft, or fixed wing aircraft which also divide in several types, like medium altitude long endurance (MALE) and high-altitude long endurance (HALE). Sadraey mainly used the already known methods of aircraft design. In this publication only battery or fuel powered drones are considered. This publication is used to add or substitute some equations and variables which do not exist for or differ from conventional aircraft of the transportation category. The downside of this guideline is that a lot of assumptions and guesses need to be made.

1.5 Structure of the Work

This thesis consists of 9 chapters. The structure of this work is as follows:

Chapter 2 In this chapter all fundamental equations and coherences for aircraft design out of previous publications are given.

Chapter 3 All requirements from possible clients, the mission defined requirements and their evaluation are given in this chapter.

Chapter 4 A trade-off study of existing drones with similar range of tasks is given in this chapter.

Chapter 5 This chapter contains the possible aircraft configurations and propulsion systems, the evaluation of the configurations and propulsion systems, and the chosen configuration and propulsion system.

Chapter 6 This chapter is about the preliminary sizing task and contains all calculations of take-off mass, fuel storage mass, operating empty mass, wing area, take-off power, and the corresponding matching charts.

Chapter 7 A draft of the fuselage cross section is given in this chapter.

Chapter 8 The task of conceptual design is given in this chapter and contains calculations of mass distribution, neutral point and dimension of the wings, size, and position of the empennage and an ascertain of the center of gravity.

Chapter 9 This chapter summarizes the thesis and gives an overview of the designed drone.

Chapter 10 This chapter provides a conclusion of this thesis and an assessment of how good the adjusted methods of aircraft design apply to designing a drone. This chapter also contains recommendations to future work on this subject.

Appendix A Extracts from literature are collected in this appendix.

Appendix B The table of the trade-off study about drones is shown in this appendix.

Appendix C The database of motor glider for the determination of empty weight to take-off weight ratio is shown in this appendix.

The associated Microsoft Excel spreadsheet for performance calculations at the preliminary sizing stage, as well as the data of the trade-off study, and the databases for weight estimations are available at: https://doi.org/10.7910/DVN/JKKX2M

2 Fundamentals of Aircraft Design

2.1 Lecture Notes Aircraft Design by Prof. Dr.-Ing. Dieter Scholz

2.1.1 Requirements

In Chapter 1 Scholz (2015, Sec. 1.1) gives the minimum requirements that should be known at the beginning of aircraft design: Payload m_{PL}, range R, and Mach number M_{CR}. Scholz also mentions, that the Mach number is not a real requirement but treated as one for later calculations.

2.1.2 Aircraft Design Sequence

Scholz gives first considerations and more requirements needed to enter the preliminary sizing phase and describes the steps of preliminary sizing in Chapter 2. The following first ideas of the aircraft must exist: Type of configuration, expected aspect ratio of the wings, cruise Mach number and type of propulsion system. The following additional requirements are needed for the preliminary sizing: Take-off field length s_{TOFL} and landing field length s_{LFL}. (Scholz 2015, Sec. 2.1)

The applicable given steps of preliminary sizing are as follows (Scholz 2015, Sec. 2.1 and 2.2):

- Step 1: Definition of all requirements, sorting, and evaluation of all requirements
- Step 2: Perform a trade-off study with comparable designed aircraft
- Step 3: Choose an aircraft configuration
- Step 4: Choose a propulsion system
- Step 5: Execute the preliminary sizing method
- Step 6: a) Draw a fuselage cross section
- Step 7: a) Define wing parameters
- Step 9: a) Design of the horizontal and vertical tail
- Step 10: b) Calculation of aircraft mass and position of center of gravity
  c) Analyze the results from b)
  d) If the center of gravity is not suitably placed or within permissible range, the arrangement of the components needs to be adjusted
- Step 16: c) Preparation of a table with all generated aircraft parameters

2.1.3 Preliminary Sizing

The next interesting chapter is Chapter 5. It deals with equations for the preliminary sizing (Scholz 2015, Sec. 5):

$$u = \frac{m_F + m_{PL}}{m_{MTO}} = 1 - \frac{m_{OE}}{m_{MTO}} \tag{2.1}$$

Equation (2.1) describes the relative useful load *u* as the ratio of useful load, which is the sum of the fuel mass m_F and payload mass m_{PL}, and maximum take-off mass m_{MTO}, or as the subtraction of 1 and the ratio of operating empty mass m_{OE} and maximum take-off mass m_{MTO}. This equation leads also to the "first rule of aircraft design" as it is called by Scholz, and is given in Equation (2.2):

$$\frac{m_F + m_{PL} + m_{OE}}{m_{MTO}} = 1 \tag{2.2}$$

Scholz assumes the first value for the zero-lift drag $C_{D,0}$ in the preliminary sizing stage as 0,02 (Scholz 2015, Sec. 5.4).

An equation, here Equation (2.3), to calculate the lift coefficient C_L at a certain speed V with the maximum lift coefficient $C_{L,max}$ and the stall speed V_S is given in Section 5.4:

$$C_L = C_{L,max}\left(\frac{V_S}{V}\right)^2 \tag{2.3}$$

Scholz (2015, Sec. 5.10) gives an equation to calculate the wing area:

$$S_W = m_{MTO} / \left(\frac{m_{MTO}}{S_W}\right) \tag{2.4}$$

Equation (2.4) gives the wing area S_W calculated with the maximum take-off mass m_{MTO} and the wing loading (m_{MTO}/S_W).

2.1.4 Wing Design

Chapter 7 covers wing design and Scholz (2015) gives the following equations:

$$A = \frac{b^2}{S} \tag{2.5}$$

Equation (2.5) gives the aspect ratio A with the span b and the area S.

Scholz (2015, Sec. 7.3) mentions that braced wings can be constructed with approximately 30% less weight than cantilever wings, but braced wings have an additional interference drag, which makes them only useful for aircraft with a cruise speed of 200 knots and less. A taper ratio λ of 0.45 is suggested for a best approximation of an elliptical lift distribution, when the sweep angle φ is 0.

2.1.5 Mass and Center of Gravity

Scholz (2015, Sec. 10.1) depicts a method to predict the masses of mass groups referring to Roskam V in three steps. The input values that need to be know are the operating empty mass m_{OE} and a mass breakdown of a similar designed aircraft like the ones that can be found in Roskam V Appendix A. The steps are as follows:

- Step 1: Provide a mass breakdown of a similar designed aircraft.
- Step 2: Calculate the relative mass breakdown with the mass breakdown from Roskam V in relation to a reference parameter from Roskam V.
- Step 3: Calculate the masses of the mass groups by multiplying the relative break down mass with the operating empty mass m_{OE} of the new design, estimated in preliminary sizing step 5.

To determine the location of the center of gravity Scholz (2015, Sec. 10.2) explains, that the design needs to be divided into two main groups, the fuselage group, and the wing group. The fuselage group contains the fuselage, horizontal and vertical tailplane, all systems, and fuselage mounted engines, if they exist. Equation (2.6) gives the x-position of the center of gravity x_{CG}, with every mass m_i and the corresponding lever arm x_i.

$$x_{CG} = \frac{\sum m_i \cdot x_i}{\sum m_i} \tag{2.6}$$

2.1.6 Horizontal Tailplane Sizing

Scholz (2015, Sec. 11.1) bases the sizing of the tailplane on the moment equilibrium around the lateral axis. This consideration gives the sum of moments around the center of gravity in a simplified form as follows:

$$M_{CG} = M_W + L_W \cdot x_{CG-AC} - T \cdot z_E - L_H \cdot (l_H - x_{CG-AC}) \tag{2.7}$$

Equation (2.7) gives the sum of moments with the moment of the wing M_W, the lift of the wing L_W and the distance of center of gravity and aerodynamic center x_{CG-AC}, the thrust of the engines T and the distance of the center of thrust and the center of gravity z_E, and the lift of the horizontal tailplane L_H and the level arm of the horizontal tailplane to the center of gravity $(l_H - x_{CG-AC})$.

2.1.7 Vertical Tailplane Sizing

To determine the vertical tailplane area Scholz (2015, Sec. 11.3) gives the following equation:

$$S_V = \frac{N_E + N_D}{\frac{1}{2}\rho V_{MC}^2 \cdot \delta_F \left[\frac{c_{L,\delta}}{(c_{L,\delta})_{theory}}\right] \cdot (c_{L,\delta})_{theory} \cdot K' \cdot K_\Lambda \cdot l_V} \tag{2.8}$$

with

$$V_{MC} = 1{,}2 \cdot V_S \tag{2.9}$$

$$\delta_F \leq 25° \tag{2.10}$$

$$N_E = \frac{T_{TO}}{n_E} \cdot y_E \tag{2.11}$$

N_D for fixed pitch propeller:

$$N_D = 0{,}75 \cdot N_E \tag{2.12}$$

$$K_\Lambda = (1 - 0{,}08 \cdot \cos^2 \varphi_{25}) \cdot \cos^{3/4} \varphi_{25} \tag{2.13}$$

Equations (2.8) through (2.13) calculate the area of the vertical tailplane S_V considering two momenta around the vertical axis caused by engine failure on one side and symmetrically positioned engines, the momentum caused by the running engine N_E and the momentum caused by the failed engine N_D. Equations (2.8) through (2.13) also contain the air density ρ, the minimum control speed V_{MC}, the deflection angle of the rudder δ_F in radiant, an empirical correction factor for lift effictivenes $\frac{c_{L,\delta}}{(c_{L,\delta})_{theory}}$, given in Appendix A, Figure A.1, the theoretical lift effectiveness $(c_{L,\delta})_{theory}$, given in Appendix A, Figure A.1, an empirical correction factor for nonlinear effects K', given in Appendix A, Figure A.2, an empirical correction factor that takes the sweep angle into account K_Λ, and the lever arm of the vertical tailplane l_V.

2.2 Design of Unmanned Aerial Systems by Dr. Mohammad H. Sadraey

2.2.1 Battery Weight

To calculate the weight of the battery Sadraey (2020, Sec. 2.7) defines an energy density of the battery E_D with the output power P, the flight time t, and the battery mass m_B as follows:

$$E_D = \frac{Pt}{m_B} \tag{2.14}$$

The battery mass m_B will be:

$$m_B = \frac{Pt}{E_D} \tag{2.15}$$

Table 2.1 Typical values for number of parameters for a fixed-wing unmanned aerial vehicle (UAV). (Sadraey 2020, Sec. 2.7)

No	Parameter	Typical values	Name
1	C_{D_0}	0,02 – 0,03	Zero-lift drag coefficient – retractable landing gear
2	C_{D_0}	0,03 – 0,045	Zero-lift drag coefficient – fixed landing gear
3	AR	5 – 20	Aspect ratio (AR)
4	C_{L_c}	0,2 – 0,5	Cruise lift coefficient
5	$C_{L_{\max}}$	1,2 – 1,6	Maximum lift coefficient
6	e	0,6 – 0,9	Oswald efficiency factor
7	η_P	0,6 – 0,8	Prop efficiency
8	$(C_L/C_D)_{\max}$	6 – 10	Maximum lift-to-drag ratio – fixed landing gear
9	$(C_L/C_D)_{\max}$	8 – 16	Maximum lift-to-drag ratio – retractable landing gear

For further value estimations of parameters, Sadraey (2020, Sec. 2.7) gives ranges for fixed-wing Unmanned Aerial Vehicles (UAV) shown in Table 2.1.

2.2.2 Empty Weight

Due to lack of geometry and sizing in this design phase Sadraey (2020, Sec. 2.8) states, that the empty weight can only be considered with an empirical solution as follows:

$$\frac{W_E}{W_{TO}} = a \cdot W_{TO} + b \tag{2.16}$$

The empirical Equation (2.16) gives the empty weight fraction $\frac{W_E}{W_{TO}}$ with a variable a and a variable b. Those variables need to be determined with statistical values from existing aircraft which are similar in design.

2.2.3 Wing and Engine Sizing

In Section 2.9 Sadraey (2020) gives the Equations (2.17) through (2.30) to calculate performance requirements that are used to draw a matching chart and find a fitting design point.

Stall

$$\left(\frac{W}{S}\right)_{V_S} = \frac{1}{2}\rho V_S^2 C_{L_{\max}} \tag{2.17}$$

Equation (2.17) calculates the wing loading at stall performance $\left(\frac{W}{S}\right)_{V_S}$ with the air density ρ, the stall speed V_S, and the maximum lift coefficient $C_{L_{\max}}$.

Maximum Speed

$$\left(\frac{W}{P_{SL}}\right)_{V_{\max}} = \frac{\eta_P}{\frac{1}{2}\rho_0 V_{\max}^3 C_{D_0}\frac{1}{\left(\frac{W}{S}\right)} + \frac{2K}{\rho\sigma V_{\max}}\left(\frac{W}{S}\right)} \tag{2.18}$$

with

$$K = \frac{1}{\pi \cdot e \cdot AR} \tag{2.19}$$

$$\sigma = \frac{\rho}{\rho_0} \tag{2.20}$$

Equations (2.18) through (2.20) calculate the weight to power ratio at maximum speed performance $\left(\frac{W}{P_{SL}}\right)_{V_{\max}}$ with the propeller efficiency η_P, the air density at sea level ρ_0, the maximum speed $V_{\max}$, the drag at zero lift C_{D_0}, the wing loading $\left(\frac{W}{S}\right)$ as a variable, the induced drag factor K, the air density of the surrounding air ρ, and the relative air density σ.

The induced drag factor K can be calculated with Equation (2.19) with the Oswald span efficiency factor e and the wing aspect ratio AR.

Take-off Run

$$\left(\frac{W}{P}\right)_{S_{TO}} = \frac{1 - \exp\left(0{,}6\rho g C_{D_G} S_{TO} \frac{1}{W/S}\right)}{\mu - \left(\mu + \frac{C_{D_G}}{C_{L_R}}\right)\left[\exp\left(0{,}6\rho g C_{D_G} S_{TO} \frac{1}{W/S}\right)\right]} \cdot \frac{\eta_P}{V_{TO}} \tag{2.21}$$

with

$$C_{D_G} = (C_{D_{TO}} - \mu C_{L_{TO}}) \tag{2.22}$$

$$V_{TO} = 1{,}1 V_S \tag{2.23}$$

$$C_{L_{TO}} = C_{L_C} + \Delta C_{L_{flapTO}} \tag{2.24}$$

$$C_{D_{TO}} = C_{D_{0_{TO}}} + K C_{L_{TO}}^2 \tag{2.25}$$

$$C_{D_{0_{TO}}} = C_{D_0} + C_{D_{0_{LG}}} + C_{D_{0_{flapTO}}} \tag{2.26}$$

$$C_{L_R} = \frac{C_{L_{\max}}}{1{,}21} \tag{2.27}$$

Equations (2.21) calculate the weight to power ratio at take-off performance $\left(\frac{W}{P}\right)_{S_{TO}}$ with the air density ρ, the gravitational constant g, the ground drag coefficient C_{D_G}, the take-off distance S_{TO}, the friction coefficient of the landing strip μ, the rotation lift coefficient C_{L_R}, the propeller efficiency η_P, and the take-off speed V_{TO}. The wing loading W/S is the variable of this equation.

The ground drag coefficient C_{D_G} is calculated with the take-off drag coefficient $C_{D_{TO}}$, the friction coefficient of the landing strip μ, and the take-off lift coefficient $C_{L_{TO}}$ as seen in Equation (2.22).

The take-off speed V_{TO} is calculated as 10% faster than the stall speed V_S as seen in Equation (2.23).

The take-off lift coefficient $C_{L_{TO}}$ is calculated with the cruise lift coefficient C_{L_C} and the gain of lift coefficient with flaps in take-off configuration $\Delta C_{L_{flapTO}}$ as seen in Equation (2.24).

The take-off drag coefficient $C_{D_{TO}}$ is calculated with the zero-lift take-off drag $C_{D_{0_{TO}}}$, the induced drag factor K, and the take-off lift coefficient $C_{L_{TO}}$ as seen in Equation (2.25).

The zero-lift take-off drag coefficient $C_{D_{0_{TO}}}$ is the sum of zero-lift drag C_{D_0}, zero-lift drag coefficient of the landing gear $C_{D_{0_{LG}}}$, and the zero-lift drag coefficient of the flaps in take-off configuration $C_{D_{0_{flapTO}}}$ as seen in Equation (2.26).

The rotation lift coefficient C_{L_R} is calculated as the maximum lift coefficient $C_{L_{\max}}$ divided by 1,21 as seen in Equation (2.27).

Rate of Climb

$$\left(\frac{W}{P}\right)_{ROC} = \frac{1}{\frac{ROC}{\eta_P} + \sqrt{\frac{2}{\rho\sqrt{\frac{3C_{D_0}}{K}}}\left(\frac{W}{S}\right)\left(\frac{1{,}155}{(L/D)_{\max}\,\eta_P}\right)}} \tag{2.28}$$

with

$$\left(\frac{L}{D}\right)_{\max} = \left(\frac{C_L}{C_D}\right)_{\max} = \frac{1}{2\sqrt{K \cdot C_{D_0}}} \tag{2.29}$$

Equation (2.28) calculates the weight to power ratio of the climb performance $\left(\frac{W}{P}\right)_{ROC}$ with the rate of climb ROC, the propeller efficiency η_P, the air density ρ, the zero-lift drag coefficient C_{D_0}, the induced drag factor K, and the maximum lift to drag ratio $\left(\frac{L}{D}\right)_{\max}$. The wing loading $\left(\frac{W}{S}\right)$ is set as a variable.

The maximum lift to drag ratio $\left(\frac{L}{D}\right)_{\max}$ can be calculated with the induced drag factor K and the zero-lift drag coefficient C_{D_0} as seen in Equation (2.29).

Absolute Ceiling

$$\left(\frac{W}{P_{SL}}\right)_{AC} = \frac{\sigma_{AC}}{\sqrt{\frac{2}{\rho_{AC}\sqrt{\frac{3C_{D_0}}{K}}}\left(\frac{W}{S}\right)\left(\frac{1{,}155}{(L/D)_{\max}\,\eta_P}\right)}} \tag{2.30}$$

Equation (2.30) calculates the weight to power ratio of the performance at absolute ceiling $\left(\frac{W}{P}\right)_{AC}$ where the rate of climb ROC is 0, with the relative air density at absolute ceiling σ_{AC}, the propeller efficiency η_P, the air density at absolute ceiling ρ_{AC}, the zero-lift drag coefficient C_{D_0}, the induced drag factor K, and the maximum lift to drag ratio $\left(\frac{L}{D}\right)_{\max}$. The wing loading $\left(\frac{W}{S}\right)$ is set as a variable.

The maximum lift to drag ratio $\left(\frac{L}{D}\right)_{\max}$ can be calculated with the induced drag factor K and the zero-lift drag coefficient C_{D_0} as seen in Equation (2.29).

Matching Chart

With the Equations (2.17), (2.18), (2.21), (2.28), and (2.30) a matching chart can be plotted like the example in Figure 2.1 below.

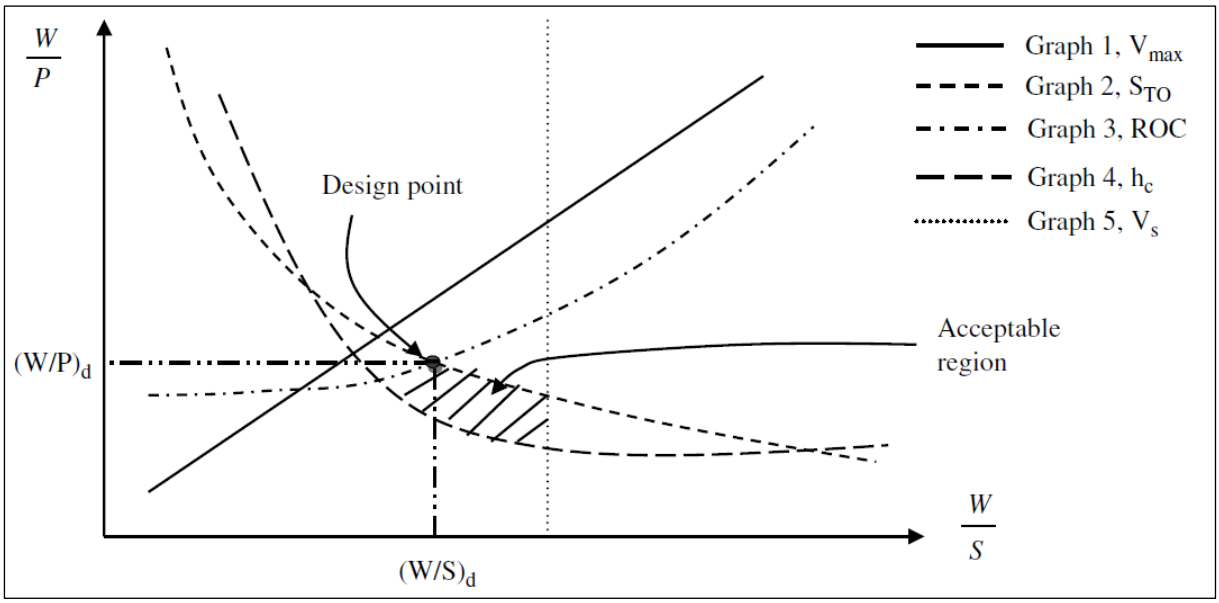

Figure 2.1 Example of a matching chart (Sadraey 2020, Sec. 2.9)

As it can be seen in Figure 2.1, the performance graphs of the maximum speed $V_{\max}$, take-off S_{TO}, rate of climb ROC, ceiling h_C, and stall speed V_S are plotted with the wing loading (W/S) as variable on the x-axis and the weight to power ratio (W/P) on the y-axis. The design point is defined in the acceptable area with a compromise of maximum weight to power ratio and maximum wing loading, and the value of the wing loading at the design point $(W/S)_d$ and power ratio at the design point $(W/P)_d$ can be determined.

Engine Power

For the calculation of engine power P with the take-off weight W_{TO} and the power ratio at the design point $(W/P)_d$, Equation (2.31) is given by Sadraey (2020, Sec. 2.9).

$$P = W_{TO} / \left(\frac{W}{P}\right)_d \tag{2.31}$$

3 Requirements

3.1 Requested from Possible Clients

To design a suitable product for a variety of applications like wildfire detection and search and rescue missions, but also for probing missions in the off season of fire endangerment, possible clients for the drone service were surveyed and interviewed to give details to their requirements. The following organizations and administrations had been contacted and shared their requirements:

- Behörde für Umwelt, Klima, Energie und Agrarwirtschaft (BUKEA) (engl.: Administration of Environment, Climate, Energy and Agriculture) and Institut für Hygiene und Umwelt (HU) (engl.: Institute of Hygiene and Environment) Hamburg
- Bundesamt für Bevölkerungsschutz und Katastrophenhilfe (BBK) (engl.: Federal Agency of Civil Protection and Disaster Relief)
- Maltester Hilfsdienst e.V. Diözese und Bezirk Hamburg (engl.: Order of Malta Relief Agency Diocese and District Hamburg)

The BUKEA and HU requested the following sensors and cameras:

- Multispectral camera:
  - wavelength 442,2 nm to 2202,4 nm
  - band width 21 nm to 185 nm, band 1 -12
  - resolution of 10 m, 20 m, 60 m
- Oil detection
  - Detectable with IR imaging
- Algae identification
- Water quality measurement

The BBK requested the following sensors, cameras, and system requirements:

- High resolution RGB- and thermal cameras for recognition of persons and vehicles within the mission area
- High accuracy of fire localization
- Good visibility in the airspace due to other operating systems and aircraft inside the mission area
  - Leads to a needed detect and avoid system (DAA system)

The Malteser Hilfsdienst requested the following sensors, cameras, and system requirements:

- RGB-camera with a resolution of at least 4K
  - Ground resolution of 1 cm/pixel
- Thermal camera with a resolution of at least 512 pixels
- IR-camera for night operation
- AI aided evaluation of abnormalities
  - Fire spreading
  - Oil contamination starting from 1 m^2
- Com-systems with 4/5G mobile network standard
  - Industry standard encryption
  - Data send directly to aid forces or network of the aid forces (headquarter)
- Networkpod to establish communication infrastructure for aid organizations
- Detect and avoid system

3.2 Definition and Evaluation of Requirements

The following requirements had been defined as the main design driving ones and are given in the order of most significance on top:

1. Propulsion: Hydrogen fuel cell and electric motor
2. Operating time: about 24 to 30 hours
3. Cruise speed: 100 to 120 km/h
4. Payload weight: 8 to 10 kg
5. Cruise level: 300 m higher than tree line
6. Wing:
   a. Span: < 5 m
   b. High aspect ratio
7. Maximum Speed: 200 km/h
8. Rate of climb: 300 m/min
9. Range: 2400 to 3600 km
10. Landing gear: optional

A hydrogen fuel cell as power supply was chosen, due to less environmental impact than a combustion engine, like greenhouse and harmful gases, and noise. To keep operating costs in means of fleet size low, a flight time of 24 to 30 hours was chosen. The cruise speed is chosen to be a significant factor of the area that can be patrolled during operation and furthermore, to get to an operation area, or a spotted fire quite quick a maximum speed was chosen for short travel distances and brief time spans. As a Medium Altitude Long Endurance (MALE) drone, the cruise altitude should not be too high to stay below commercial aviation and avoid the

need of flight plans and air traffic control. The range of the platform will be a result of speed and endurance and therefore is a subordinated requirement. The wings should provide a decent amount of lift, but also generate a low amount of induced drag, so a high aspect ratio should be chosen. Also, the platform should fit in existing infrastructure, so a maximum wingspan of 5 meters was chosen. Due to lack of federal requirements about the rate of climb, the value was chosen as a reasonable guess to get to cruise altitude in a meaningful time. To get rid of a heavy landing gear a solution like a ground-based rail and sled landing and take-off system could be possible.

3.3 Examples of Suitable Systems and Payload

3.3.1 Payload

Considering the requested requirements of Section 3.1 the WESCAM MX-8 camera is selected as payload. Telemeter (2023) gives the specifications of the MX-8 shown in Table 3.1.

Table 3.1 Specifications of the MX-8 camera

Thermal imager resolution:	640 x 480 pixels
Color camera resolution:	1280 x 720 pixels
Laser rangefinder:	Type Class I
Laser illuminator:	Type Class IIIb
Weight:	6,8 kg
Diameter:	211 mm
Hight:	262,5 mm
Power consumption:	65 W

3.3.2 Flight Control Systems

For maneuvering the drone, to detect and avoid obstacles or other aircraft, flight control systems need to be chosen. For this project, the following systems are considered:

Autopilot

Table 3.2 Specifications of Veronte Autopilot 4x

Weight:	750 g
Size:	128 x 70 x 84 mm
Power consumption:	29 W

Table 3.2 shows the specifications of the Veronte Autopilot 4x given by Embention (2023).

Detect and Avoid

Table 3.3 Specifications of detect and avoid systems

Casia X (Cameras)	
Weight:	2400 g
Size:	103 x 168 x 52 mm
Power consumption:	65 W
IntuVue RDR-84K (Radar)	
Weight:	0,7 kg
Size:	226 x 125 x 43 mm
Power consumption:	60 W
PING-200SR (ADS-B Transponder)	
Weight:	76 g
Size:	91 x 57 x 17 mm
Power consumption:	2 W

Table 3.3 shows the specifications for the Casia X detect-and-avoid system given by Iris Automation (2023), the IntuVue RDR-84K radar system given by Honeywell (2023), and the PING-200SR ADS-B transponder given by Northwest UAV (2023).

GPS

As GPS antennas the Trimble AX940I antennas from Trimble are chosen. The specifications distributed by TerrisGPS (2023) can be found in Table 3.4.

Table 3.4 Specifications of Trimble AX940I

Weight:	0,66 kg
Size:	221 x 218 x 52 mm
Power consumption:	3 W

Transmission System

To be able to transmit the video footage of the payload camera, a transmission system is needed. For this drone, the transmission system Sky Drone Link 3 from Sky Drone is used. The specifications of this system, provided by Sky Drone (2023), can be seen in Table 3.5.

Table 3.5 Specifications of Sky Drone Link 3

Weight:	228 g
Size:	N/A
Power consumption:	10 W

3.3.3 Power Supply

Fuel Cells

To generate electrical power, fuel cells are needed to convert the chemical energy of hydrogen and oxygen of the air. The specifications of the fuel cells from H3 Dynamics (2023) can be found in Table 3.6.

Table 3.6 Specifications of fuel cells from H3 Dynamics

A-2000	
Rated power:	2.000 W
Weight:	3 kg
Size:	339 x 143 x 172 mm
A-1200 HV	
Rated power:	1.200 W
Weight:	2,1 kg
Size:	194 x 127 x 193 mm
A-800	
Rated power:	800 W
Weight:	1,23 kg
Size:	214 x 123 x 130 mm
A-300	
Rated power:	300 W
Weight:	0,72 kg
Size:	122 x 123 x 112 mm

Hydrogen Cylinders

To store the hydrogen needed for the fuel cells, the A-Series gas cylinders from H3 Dynamics were selected. The specifications are provided by H3 Dynamics (2023) and can be found in Table 3.7.

Table 3.7 Specifications of the hydrogen gas cylinders

A5	
Diameter:	152 mm
Length:	395 mm
Weight:	1,65 kg
Electrical energy:	2000 Wh
A9	
Diameter:	173 mm
Length:	528 mm
Weight:	2,65 kg
Electrical energy:	3600 Wh
A12	
Diameter:	196 mm
Length:	532 mm
Weight:	3,3 kg
Electrical energy:	4800 Wh
A20	
Diameter:	230 mm
Length:	655 mm
Weight:	7,05 kg
Electrical energy:	8000 Wh

3.4 Mission Definition

The mission definition is not required for the design approach of this thesis, because the fuel mass of hydrogen is negligible compared to the mass of the cylinders it is stored in. To get an idea of the mission the drone is used for, two missions are defined, nevertheless.

Figure 3.1 shows a loiter-mission. In a loiter-mission, the drone starts, climbs to its cruise altitude, flies to its operating site and circles around the operating site to provide pictures and life video footage of the site. When the operation on site is over, or the hydrogen is depleted to a level where the drone must return to its base, the drone starts the cruise back to the base, descents, and lands.

Figure 3.2 shows a search-mission. In a search-mission the operating site is not spatially circumscribed. The drone searches in a wider area for wildfires or persons, after the drone started, climbed to its cruise altitude and flies to the search area. At the search area photo and video footage is provided. When the search is done, or the hydrogen is depleted to a level where the drone must return to its base, the drone starts the cruise back to the base, descents, and lands.

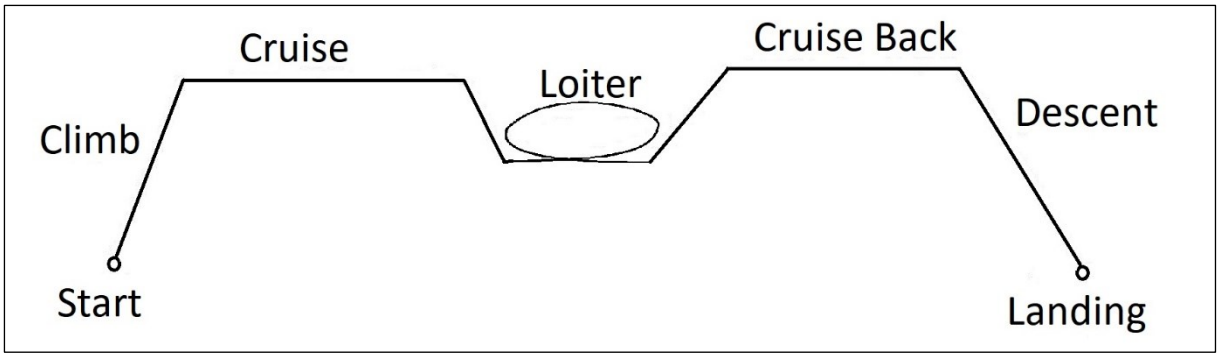

Figure 3.1 Definition of loiter-mission

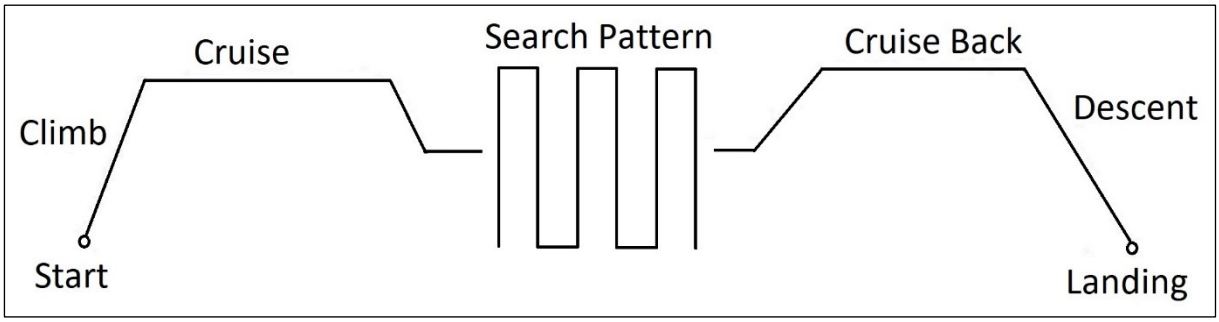

Figure 3.2 Definition of search-mission

4 Trade-off Study

To get an idea of how a drone with the determined requirements can look like and what the further specifications could be like, a trade-off study was done with 73 available military and civil drones.

Figures 4.1 through 4.4 show different diagrams of the trade-off study with the groupings around the specified design goal. To find comparable design approaches, the drones within the group near the design goal in the diagrams are looked at with more detail.

Figure 4.1 shows a diagram with the payload versus the range of the considered drones and the design goal. The grouping around the design goal in this diagram are Raybird 3, Primoco UAV One 150, Flexrotor, and ORYX.

Figure 4.2 shows a diagram with the range versus the endurance of the considered drones and the design goal. The grouping around the design goal in this diagram are Raybird 3, Flexrotor, and ORYX.

Figure 4.3 shows a diagram with the speed versus the endurance of the considered drones and the design goal. The grouping around the design goal in this diagram are Raybird 3, S1-V300, Flexrotor, and ORYX.

Figure 4.4 shows a diagram with the speed versus the range of the considered drones and the design goal. The grouping around the design goal in this diagram are Albatross 2.2 and The Black Swan. Raybird 3, Primoco UAV One 150, Flexrotor, and ORYX are in a wider grouping around the design goal, but considering, that the mostly operated cruise speed is less, then the design goal regroups in this second grouping.

In this chapter the five most similar existing platforms are shown and the full data of considered drones can be found in Appendix B.

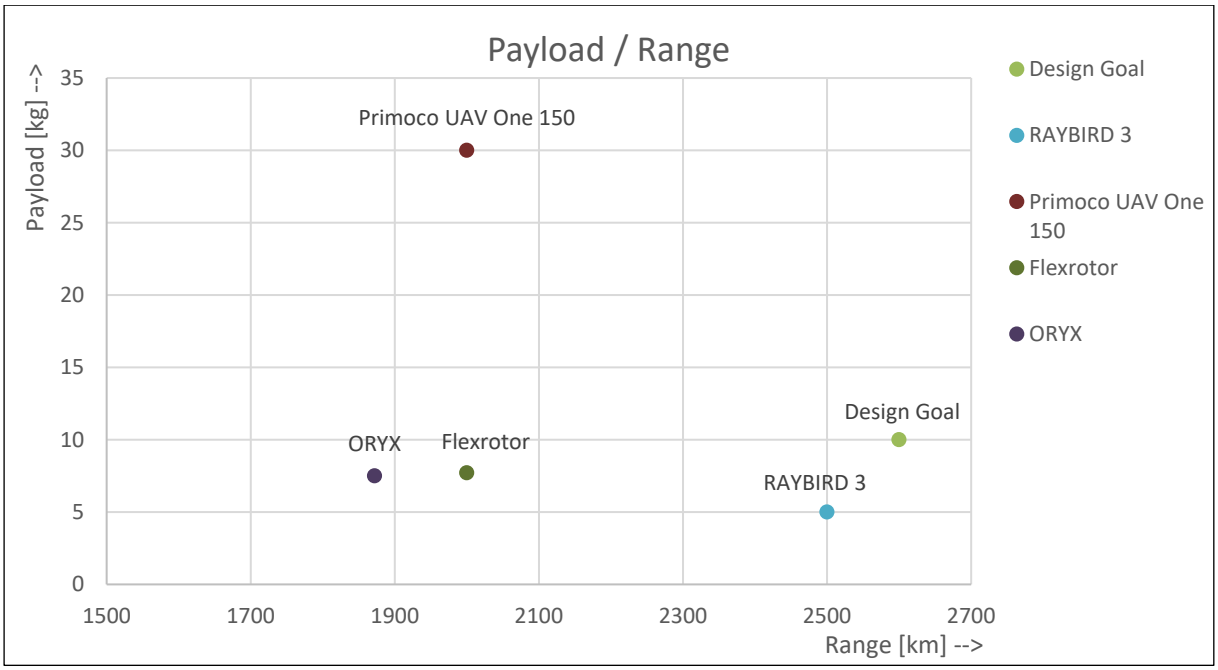

Figure 4.1 Payload / Range diagram

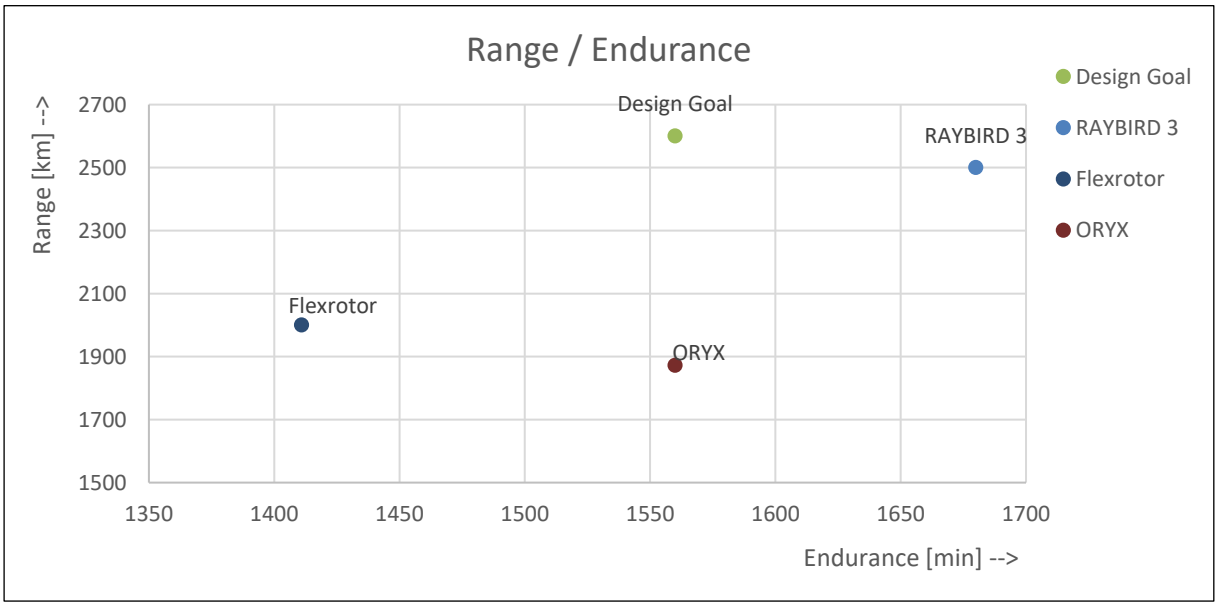

Figure 4.2 Range / Endurance diagram

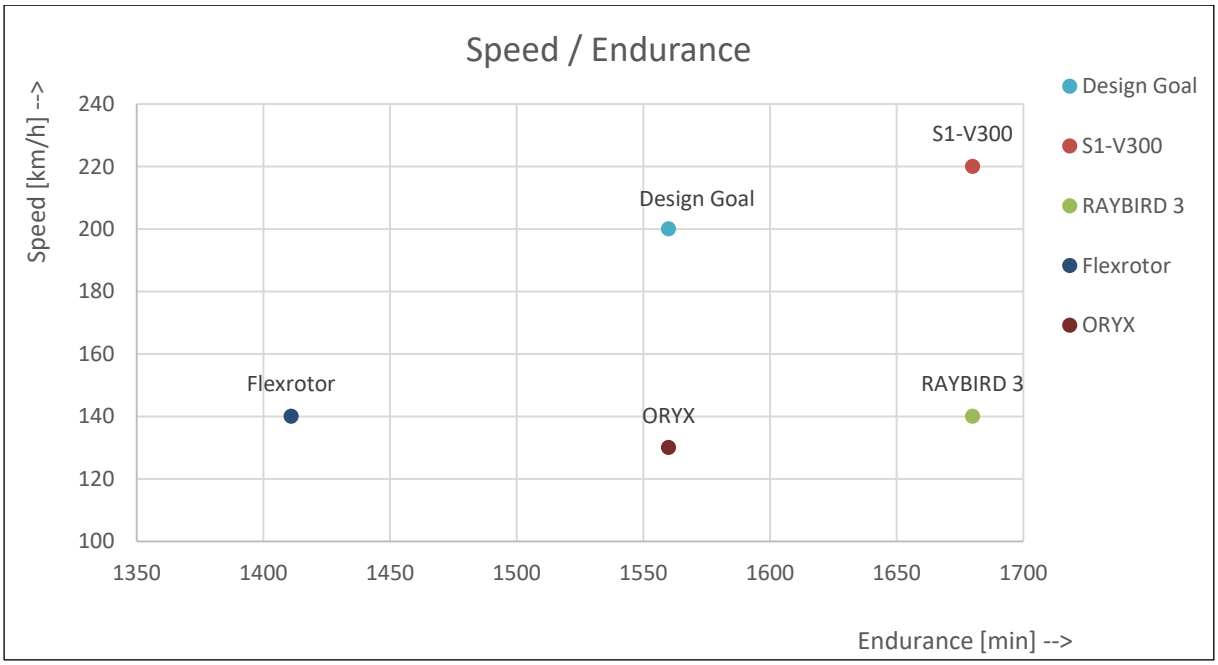

Figure 4.3 Speed / Endurance diagram

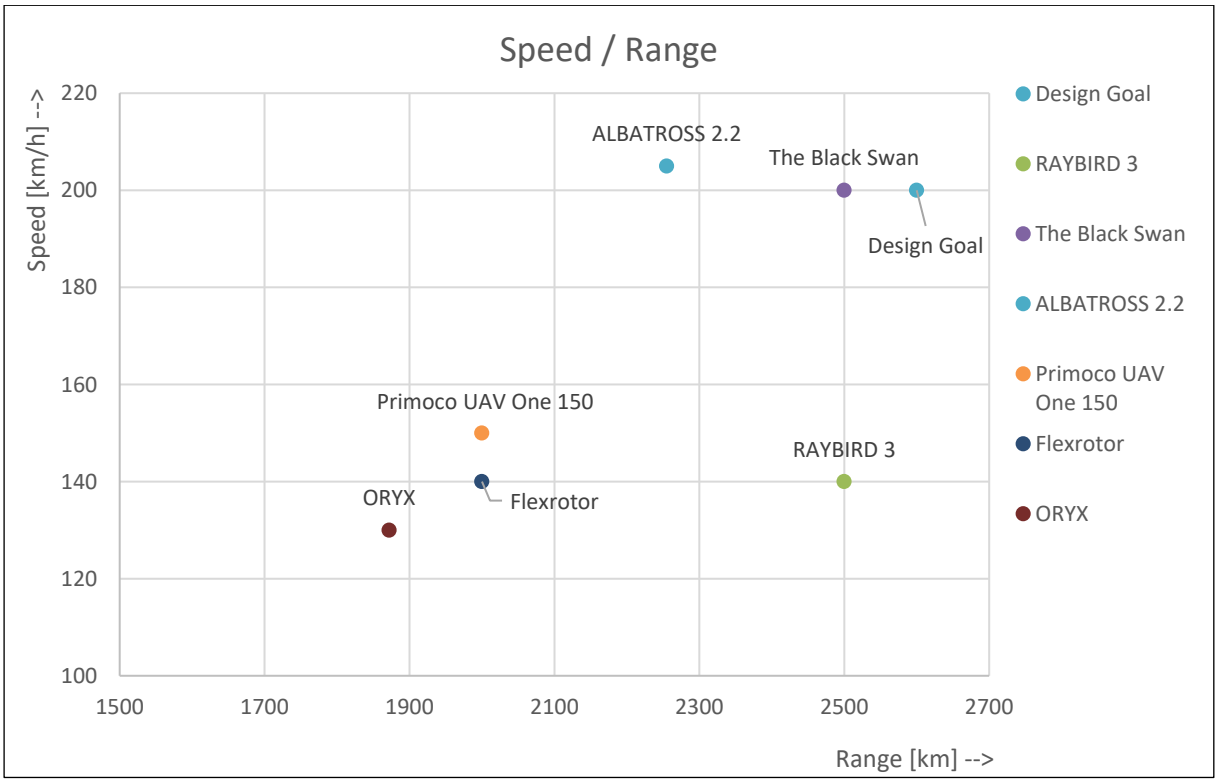

Figure 4.4 Speed / Range diagram

4.1 RAYBIRD 3

The Raybird 3 is, as seen in Figure 4.5, a fixed-wing drone with a single-prop gas powered combustion engine at the front and interchangeable payload like video cameras and radar. The Raybird 3 is distributed by Skyeton and has the following additional specifications (Skyeton 2023):

- Max. Speed: 140 km/h
- Range: 2500 km
- Endurance: up to 28 hours
- Service Ceiling: 4500 m AMSL
- Max. Payload: 5 kg
- MTOW: 21 kg
- Wingspan: 2,96 m
- Launch: Catapult
- Recovery: Parachute, airbag

Figure 4.5 Top view of the Raybird 3 (Skyeton 2023)

4.2 Flexrotor

The Flexrotor is, as seen in Figure 4.6, a fixed-wing drone with a single-prop gas powered combustion engine at the front. One specialty is, that the propeller in the front is dimensioned to function as a rotor for vertical take-off and landing with a diameter of 2,2 meters. Once in the air with enough altitude, the whole drone pivots forward for horizontal flight. This drone is a military drone for surveillance purposes and has no published payload specifications. The Flexrotor is distributed by Volatus Aerospace and has the following additional specifications (Volatus Aerospace 2023):

- Max. Speed: 140 km/h
- Range: 2000 km
- Endurance: about 23 hours (calculated with speed and range)
- Service Ceiling: 6500 m AMSL
- Max. Payload: 7,7 kg
- MTOW: 25 kg
- Wingspan: 3,0 m
- Launch: VTOL
- Recovery: VTOL

Figure 4.6 Picture of the Flexrotor (Volatus Aerospace 2023)

4.3 Primoco UAV One 150

The Primoco UAV One 150, as seen in Figure 4.7, is a fixed-wing drone with a single-prop gas powered combustion engine at the back and interchangeable payload like video cameras or a LiDAR-System. Primoco (2023) also states, that customized sensor and payload can be fitted, if required. The Primoco UAV One 150 is distributed by Primoco UAV SE and has the following additional specifications (Primoco 2023):

- Max. Speed: 150 km/h
- Range: 2000 km
- Endurance: up to 19 hours
- Service Ceiling: 3300 m AMSL
- Max. Payload: 30 kg
- MTOW: 150 kg
- Wingspan: 4,85 m
- Launch: Airstrip
- Recovery: Airstrip

Figure 4.7 Picture of the Primoco UAV One 150 (Primoco 2023)

4.4 ORYX

The ORYX, as seen in Figure 4.8, is a fixed-wing drone with a single-prop gas powered combustion engine at the front and a cargo bay that can be adapted to different payloads. The ORYX is distributed by CAT UAV and has the following additional specifications (CAT UAV 2023):

- Max. Speed: 130 km/h
- Range: about 1872 km (calculated with speed and endurance)
- Endurance: up to 26 hours
- Service Ceiling: N/A
- Max. Payload: 7,5 kg
- MTOW: 22 kg
- Wingspan: 3,0 m
- Launch: Airstrip
- Recovery: Airstrip

Figure 4.8 Picture of the ORYX in flight (CAT UAV 2023)

4.5 The Black Swan

The Black Swan, as seen in Figure 4.9, is a fixed-wing drone with a single-prop gas powered combustion engine at the front and cargo bay that is designed for parcels. The Black Swan is distributed by Dronamics and has the following additional specifications (Dronamics 2023):

- Max. Speed: 200 km/h
- Range: 2500 km
- Endurance: about 12,5 hours (calculated with range and speed)
- Service Ceiling: 6096 m AMSL
- Max. Payload: 350 kg
- MTOW: N/A
- Wingspan: 16,0 m
- Launch: Airstrip
- Recovery: Airstrip

Figure 4.9 3D-Image of The Black Swan (modified from Business Insider 2023)

5 Aircraft Configuration and Propulsion System

5.1 Aircraft Configuration

For the aircraft configuration a lot of designs can be considered. The most likely ones are shown in the list below and in Figures 5.1 and 5.2:

- Wing configuration:
  - High wing
  - Low wing
  - Mid wing
  - Blended wing body (BWB)
- Empennage:
  - T-tail
  - Cruciform tail
  - V-tail
  - Conventional tail

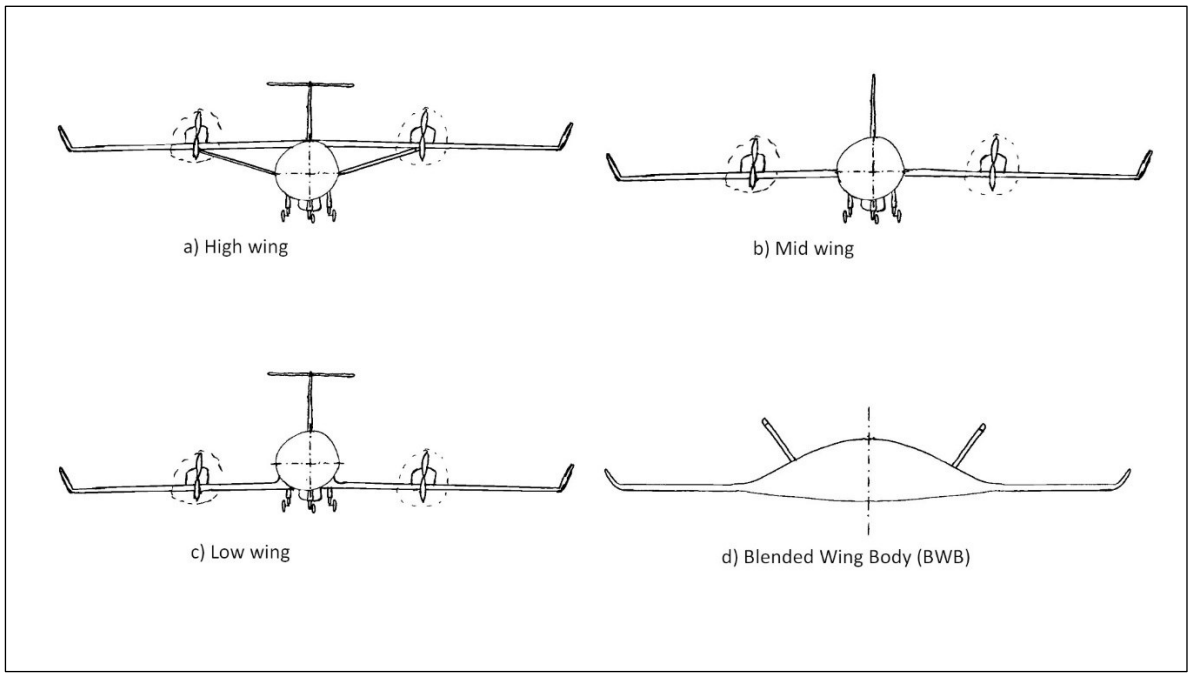

Figure 5.1 Wing configurations

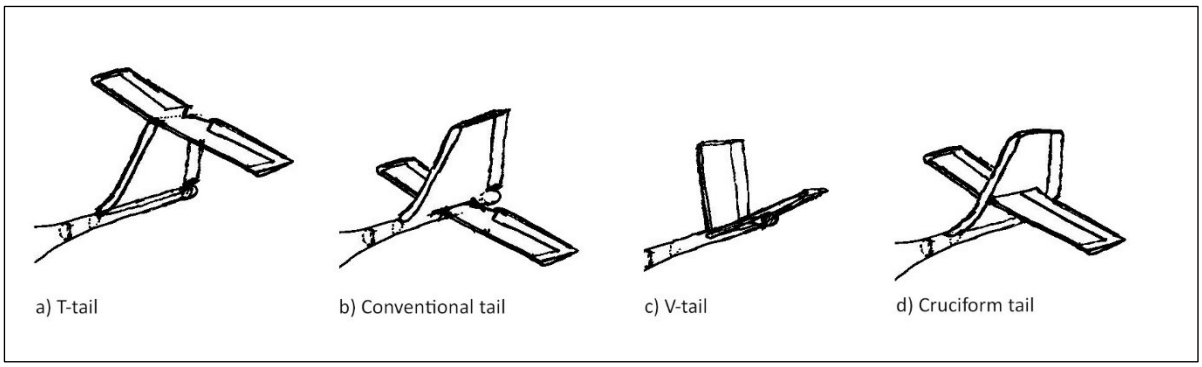

Figure 5.2 Empennage configurations

5.1.1 Vertical Position of the Wing

To evaluate the different wing configuration options, advantages, and disadvantages from Gudmundsson (2014, Sec. 4.2.1) and own perception are listed below.

High wing

Advantages

- Can be braced (less weight)
- Higher ground clearance
- Clear ground visibility for bottom mounted cameras and sensors
- Greater roll stability
- Shorter landing distance due to less ground effect
- Harder to stall
- Better L/D

Disadvantages

- Higher interference drag
- More momentum around CG
- Obstructed view in turns
- More pressure needed on the ailerons
- Longer take-off distance due to less ground effect
- Greater buffeting due to stall
- More affected by crosswinds
- Fuselage takes most loading during rough landing

Low wing

Advantages

- Less interference drag
- Less momentum around CG
- Greater visibility during turns
- Less pressure needed on the ailerons and more agile
- Shorter take-off distance due to greater ground effect
- Smoother stall with less buffeting
- Less affected by crosswinds
- Wing structure takes loading during rough landing

Disadvantages

- Less ground clearance
- Ground visibility obstructed by wings
- Less roll stability
- Longer landing distance due to greater ground effect
- Stall with less warnings
- Less rudder and elevator efficiency due to effected airflow by the wings

Mid wing

Advantages

- Less interference drag
- Compromise with ground clearance
- Good agility and good roll stability

Disadvantages

- Wing box reaches through fuselage
- Rear attachment leads to rear shifting of CG

Blended Wing Body (BWB)

Advantages
- Less drag
- Body generates more lift
- More efficient
- Low wetted area to internal volume ratio
- Space for engine integration onto the fuselage and therefore less noise

Disadvantages
- Less ground clearance
- Issues with stability
- Rear attachment of engines shifts CG to rear
- Complex flight control system required
- Less experience about design and parameters

5.1.2 Tail Configuration

To evaluate the different empennage configuration options, advantages, and disadvantages from Gudmundsson (2014, Sec. 11.3) and own perception are listed below.

T-tail

Advantages
- Endplate effect, vertical tailplane can be smaller
- Higher efficiency due to less downwash from wings
- Less tail buffeting
- Space for tail mounted engines
- Great spin recovery potential
- Less ground effect

Disadvantages
- Heavy, weight of horizontal tailplane must be carried
- Deep stall possible at high angle of attack

V-tail

Advantages

- Less interference drag
- Less tendency for rudder locking
- Less elevator deflection needed
- Less ground effect
- Engine can be mounted on top of fuselage

Disadvantages

- Complicated mechanics necessary
- Rudder deflection causes roll moment against desired turn in upright configuration
- No weight and area advantage compared to other configurations
- Greater loads and therefore more weight

Cruciform tail

Advantages

- Lighter than T-tail
- Engines can be mounted at rear
- Good spin recoverability
- Less ground effect

Disadvantages

- Bigger area needed than T-tail due to limited endplate effect
- Heavier than conventional tail due to higher torsional loads and therefore more structural reinforcement
- Elevator must be sectoral divided at the root to allow rudder to move freely
- Rudder sectional un-blanketed and reduced rudder authority in stall
- Higher interference drag
- Increased costs

Conventional tail

Advantages

- Appropriate stability and control
- Lightweight
- Wake from wings gives feedback about imminent stall
- Good stall recovery when horizontal tailplane is out of wake of wings
- Torsional loads can be inserted into the aft fuselage

Disadvantages

- Large area affected by downwash from the wings
- Rudder and vertical tail un-blanketed in stall and harder spin recovery

5.2 Propulsion System

As propulsion system a hydrogen fuel cell powered electric engine was defined as design requirement. To power the fuel cells hydrogen must be carried in gas tanks. The provided electrical energy is transferred to the systems, sensors, and engine. To provide thrust, the engine drives a propeller. The following two engine configurations were considered for this design and are shown in Figure 5.3:

- Single-prop engine at the back as a pusher
- Dual-prop engine on the wings as a tractor

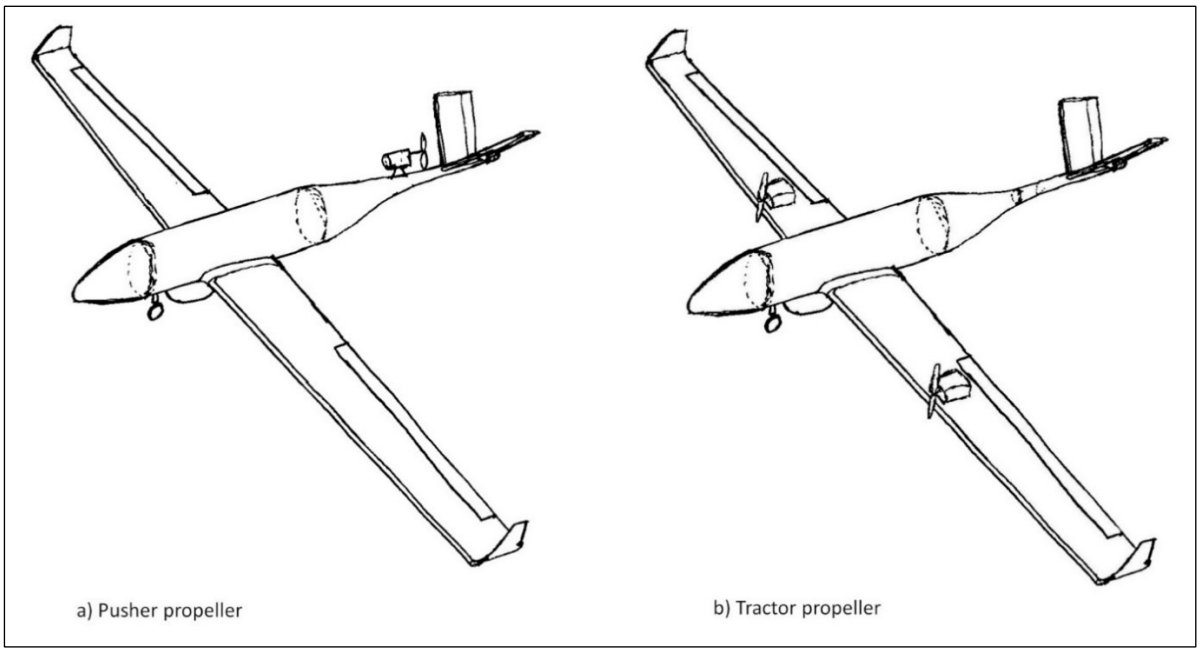

Figure 5.3 Pusher and tractor propeller configurations

For evaluation of the two options, the advantages, and disadvantages from Gudmundsson (2014, Sec. 4.2.6, Sec. 4.2.7, and Sec. 14.1.2) and own perceptions were sighted and are written in Table 5.1.

Table 5.1 Advantages and disadvantages of considered engine options

Single-prop engine at back (pusher)		*Dual-prop engine on wings (tractor)*	
Advantages	**Disadvantages**	**Advantages**	**Disadvantages**
Less drag			More drag
Less weight	No redundancy	Redundancy	More weight
	More noise	Less noise	
	Little clearance during rotation	More clearance during rotation	
	Less efficient	More efficient	
	Bigger prop-disc needed	Smaller prop-discs	
	Airflow disturbed by fuselage	Clean airflow in front	
No prop-wash around fuselage and tailplanes	More stress to the blades	Less stress to the blades	Prop-wash around fuselage and tailplanes
		Prop-wash can shorten the take-off and landing distance	
	CG is brought back		
	More difficult engine cooling	Easy engine cooling	
		Load relief on wings	
			Bigger vertical tailplane area needed for failing engine
	Limited power		
Less leverage between thrustline and CG			More leverage between thrustline and CG
	Higher risk of FOD damage	Lower risk of FOD damage	
Increased stability			Decreased stability, when in front of CG

5.3 Design Decisions

Considering the advantages and disadvantages listed in Section 5.1.1, a high wing configuration was chosen, especially due to its ability to be braced, higher ground clearance, less blind spots with bottom mounted sensors and cameras, and greater roll stability.

Considering the advantages and disadvantages listed in Section 5.1.2, a conventional tail was chosen, especially due to its provided stability and control, lightweight structure, and good stall recovery possibility.

Considering the advantages and disadvantages listed in Section 5.2, the dual-prop engine option on the wings as a tractor configuration was chosen, especially due to the given redundancy, less noise, higher efficiency, ground clearance, and load relief on the wings.

6 Preliminary Sizing

In this chapter three designs will be calculated with the assumed values shown in Table 6.1. The values for maximum speed, cruise speed, stall speed, take-off distance, rate of climb, cruise altitude, absolute ceiling, payload mass, and system power consumptions are determined as a result of requirements. The values for wing aspect ratio, Oswald factor, maximum lift coefficient, lift-to-drag ratio, zero-lift coefficient, propeller efficiency, and friction coefficient of the landing strip are determined with Table 2.1.

Table 6.1 Assumed values of the calculated designs

Input variables	**Design 1**	**Design 2**	**Design 3**
Maximum speed $V_{\max}$ [km/h]	150	150	150
Cruise speed V_C [km/h]	100	100	100
Stall speed V_S [km/h]	54	54	54
Take-off distance S_{TO} [m]	80	80	80
Rate of climb ROC [m/min]	300	300	300
Cruise altitude [m]	500	500	500
Absolute ceiling h_C [m]	4000	4000	4000
Wing aspect ratio AR [-]	**20**	**14**	**6**
Payload mass m_{PL} [kg]	10	10	10
Oswald factor e [-]	0,8	0,8	0,8
Max lift coefficient $C_{L_{\max}}$ [-]	1,2	1,2	1,2
Lift-to-drag ratio L/D [-]	**20**	**16**	**12**
Zero-lift drag coefficient C_{D_0} [-]	0,03	0,03	0,03
Propeller efficiency η_P [-]	0,8	0,8	0,8
Friction coefficient landing strip μ [-]	0,04	0,04	0,04
System power consumption P_{Sys} [W]	250	250	250

6.1 Performance Calculations

To begin the preliminary sizing, the matching charts for the designs are generated like mentioned in Section 2.2.3. In these matching charts the wing loading, and power-to-weight ratio are determined to give values for the further calculations of take-off mass, fuel storage mass, operating empty mass, wing area, and take-off power.

6.1.1 Stall

To calculate the wing loading at stall performance $\left(\frac{m}{S}\right)_{V_S}$, Equation (2.17) is expanded with the factor $(1/g)$, and the values from Table 6.1 are used. Equation (2.17) was changed due to unit conventions.

$$\left(\frac{m}{S}\right)_{V_S} = \left(\frac{W}{S}\right)_{V_S} \cdot \frac{1}{g} = \frac{1}{2}\rho V_S^2 C_{L_{\max}} \cdot \frac{1}{g}$$

With

$$\rho = 1{,}225\ \frac{\mathrm{kg}}{\mathrm{m}^3}$$
$$g = 9{,}81\ \frac{\mathrm{m}}{\mathrm{s}^2}$$

$$\left(\frac{m}{S}\right)_{V_S} = 16{,}86\ \frac{\mathrm{kg}}{\mathrm{m}^2}$$

6.1.2 Maximum Speed

To calculate the power-to-weight ratio at maximum speed performance $\left(\frac{P_{SL}}{m}\right)_{V_{\max}}$, inversed Equation (2.18) with an expansion with the factor g, Equation (2.19), Equation (2.20), and the values from Table 6.1 are used. Equation (2.18) was changed due to unit conventions.

$$\left(\frac{P_{SL}}{m}\right)_{V_{\max}} = \left(\frac{P_{SL}}{W}\right)_{V_{\max}} \cdot g = \frac{\frac{1}{2}\rho_0 V_{\max}^3 C_{D_0} \frac{1}{\left(\frac{W}{S}\right)} + \frac{2K}{\rho\sigma V_{\max}}\left(\frac{W}{S}\right)}{\eta_P} \cdot g$$

With

$$\rho_0 = 1{,}225\ \frac{\mathrm{kg}}{\mathrm{m}^3}$$
$$\rho = \rho_C = 1{,}167\ \frac{\mathrm{kg}}{\mathrm{m}^3}$$
$$g = 9{,}81\ \frac{\mathrm{m}}{\mathrm{s}^2}$$

6.1.3 Take-off Run

To calculate the power-to-weight ratio at take-off run performance $\left(\frac{P}{W}\right)_{S_{TO}}$, inversed Equation (2.21) with an expansion with the factor g, Equations (2.22) through (2.27), Equation (2.3), and the values from Table 6.1 are used. Equation (2.21) was changed due to unit conventions.

$$\left(\frac{P}{m}\right)_{S_{TO}} = \left(\frac{P}{W}\right)_{S_{TO}} \cdot g = \frac{\mu - \left(\mu + \frac{C_{D_G}}{C_{L_R}}\right)\left[\exp\left(0{,}6\rho g C_{D_G} S_{TO} \frac{1}{W/S}\right)\right]}{1 - \exp\left(0{,}6\rho g C_{D_G} S_{TO} \frac{1}{W/S}\right)} \cdot \frac{V_{TO}}{\eta_P} \cdot g$$

With

$$\begin{aligned}
\rho = \rho_0 &= 1{,}225\ \frac{\mathrm{kg}}{\mathrm{m}^3} \\
g &= 9{,}81\ \frac{\mathrm{m}}{\mathrm{s}^2} \\
C_{D_{0_{LG}}} &= 0 \\
C_{D_{0_{flapTO}}} &= 0 \\
\Delta C_{L_{flapTO}} &= 0
\end{aligned}$$

Therefore

$$\begin{aligned}
C_{L_C} &= 0{,}35 \\
C_{L_R} &= 0{,}9917 \\
C_{D_{0_{TO}}} &= 0{,}03 \\
C_{L_{TO}} &= 0{,}5468 \\
C_{D_{TO}} &= 0{,}03595 \\
C_{D_G} &= 0{,}01408 \\
V_{TO} &= 16{,}5\ \frac{\mathrm{m}}{\mathrm{s}}
\end{aligned}$$

6.1.4 Rate of Climb

To calculate the power-to-weight ratio at climb performance $\left(\frac{P}{W}\right)_{ROC}$, inversed Equation (2.28) with an expansion with the factor g, Equation (2.29), and the values from Table 6.1 are used. Equation (2.28) was changed due to unit conventions.

$$\left(\frac{P}{m}\right)_{ROC} = \left(\frac{P}{W}\right)_{ROC} \cdot g = \frac{\frac{ROC}{\eta_P} + \sqrt{\frac{2}{\rho\sqrt{\frac{3C_{D_0}}{K}}}\left(\frac{W}{S}\right)\left(\frac{1{,}155}{(L/D)_{\max}\,\eta_P}\right)}}{1} \cdot g$$

With

$$\rho = \rho_0 = 1{,}225\ \frac{\mathrm{kg}}{\mathrm{m}^3}$$

$$g = 9{,}81\ \frac{\mathrm{m}}{\mathrm{s}^2}$$

The calculations with Equation (2.29) gives the values for $(L/D)_{\max}$ shown in Table 6.2.

Table 6.2 Values of the maximum lift-to-drag ratio of the design approaches

	Design 1	**Design 2**	**Design 3**
$\left(\frac{L}{D}\right)_{\max}$	20,47	17,12	11,21

6.1.5 Absolute Ceiling

To calculate the power-to-weight ratio for the performance at absolute ceiling $\left(\frac{P}{W}\right)_{AC}$, inversed Equation (2.30) with an expansion with the factor g, and the values from Table 6.1 are used. Equation (2.30) was changed due to unit conventions.

$$\left(\frac{P_{SL}}{m}\right)_{AC} = \left(\frac{P_{SL}}{W}\right)_{AC} \cdot g = \frac{\sqrt{\frac{2}{\rho_{AC}\sqrt{\frac{3C_{D_0}}{K}}}\left(\frac{W}{S}\right)\left(\frac{1{,}155}{(L/D)_{\max}\,\eta_P}\right)}}{\sigma_{AC}} \cdot g$$

With

$$\rho_{AC} = 0{,}819$$
$$\sigma_{AC} = 0{,}6686$$
$$g = 9{,}81\ \frac{\mathrm{m}}{\mathrm{s}^2}$$

6.1.6 Matching Charts

With the equations and values mentioned in Section 6.1 the matching charts can be plotted. Figure 6.1 shows the matching chart for Design 1 with the design point at a wing loading of $(m/S)_{DP} = 16{,}858\ \mathrm{kg/m^2}$ and a power-to-weight ratio of $(P/m)_{DP} = 100{,}31\ \mathrm{W/kg}$. Figure 6.2 shows the matching chart for Design 2 with the design point at a wing loading of $(m/S)_{DP} = 16{,}858\ \mathrm{kg/m^2}$ and a power-to-weight ratio of $(P/m)_{DP} = 101{,}05\ \mathrm{W/kg}$. Figure 6.3 shows the matching chart for Design 3 with the design point at a wing loading of $(m/S)_{DP} = 16{,}858\ \mathrm{kg/m^2}$ and a power-to-weight ratio of $(P/m)_{DP}$ 104,37 W/kg.

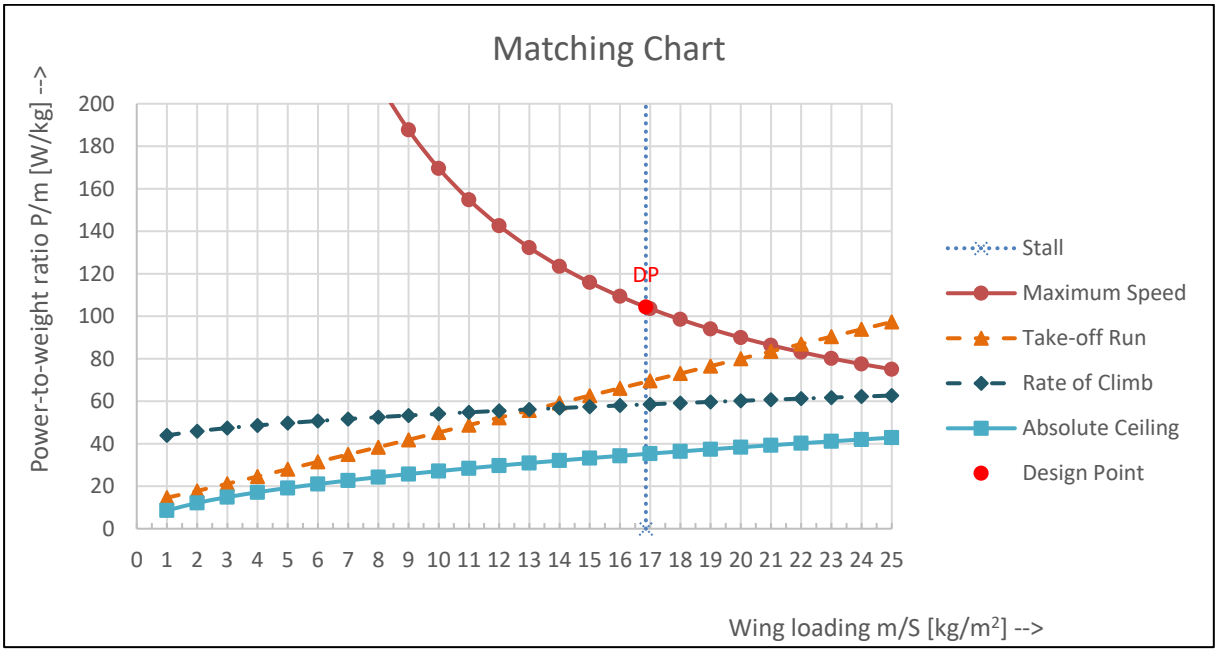

Figure 6.1 Matching chart for Design 1

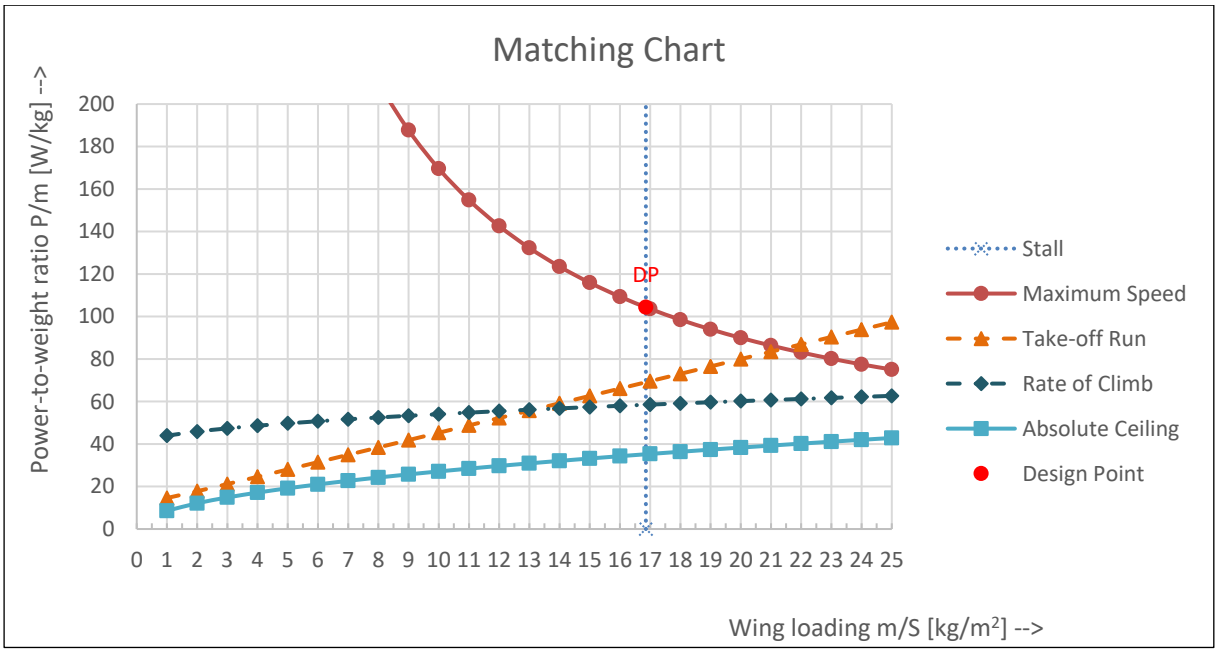

Figure 6.2 Matching chart for Design 2

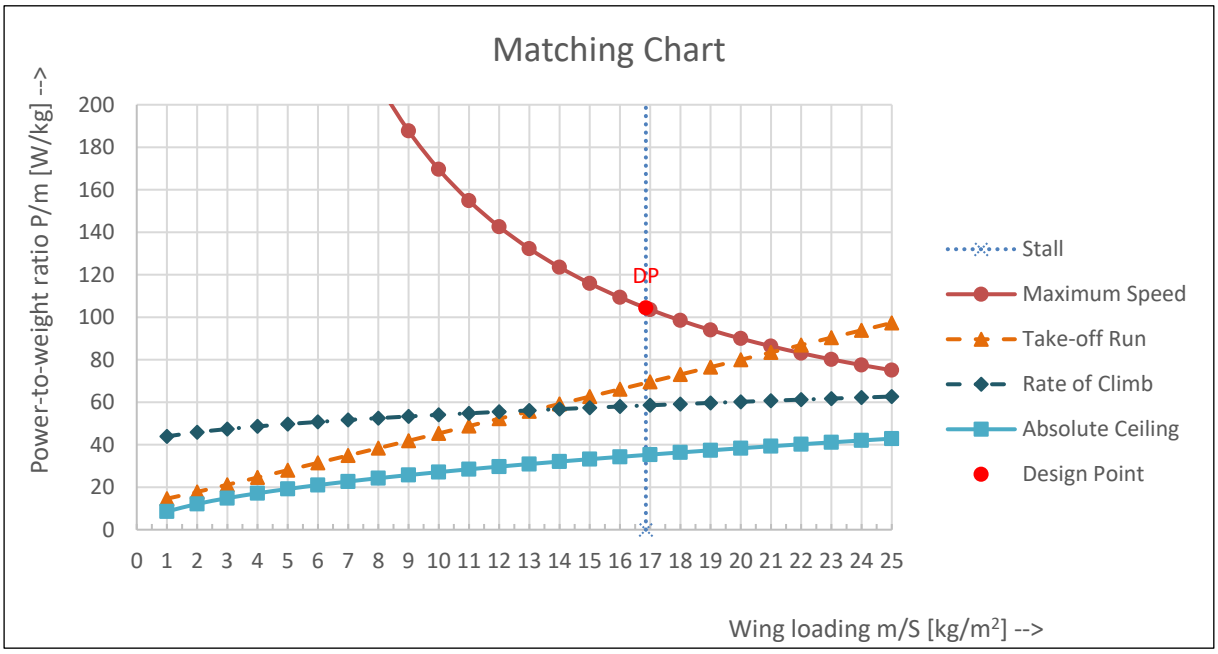

Figure 6.3 Matching chart for Design 3

6.2 Take-off Mass

All masses have an influence on each other, even more when the maximum take-off mass m_{TO} is not defined prior but is the result of a numeric extreme value calculation. The masses therefore cannot be calculated separately, but with a numeric extreme value calculation, which updates the mass fractions and the take-off mass repeatedly until the extreme value is reached. In this thesis the maximum of flight time should be reached. After the flight time

cannot be improved, the calculation stops, and the take-off mass is determined. The numeric extreme value calculation is done with Microsoft Excel.

Figure 6.4 shows the increase of take-off mass over the increase of flight endurance of an example platform, in this case the maximum flight time would be 10,74 hours. This figure also shows that an increase of flight time off a certain point comes along with a massive increase of weight. That leads to an approach in which not the maximum flight time is considered for the designs, but a little less to get a much lower take-off mass.

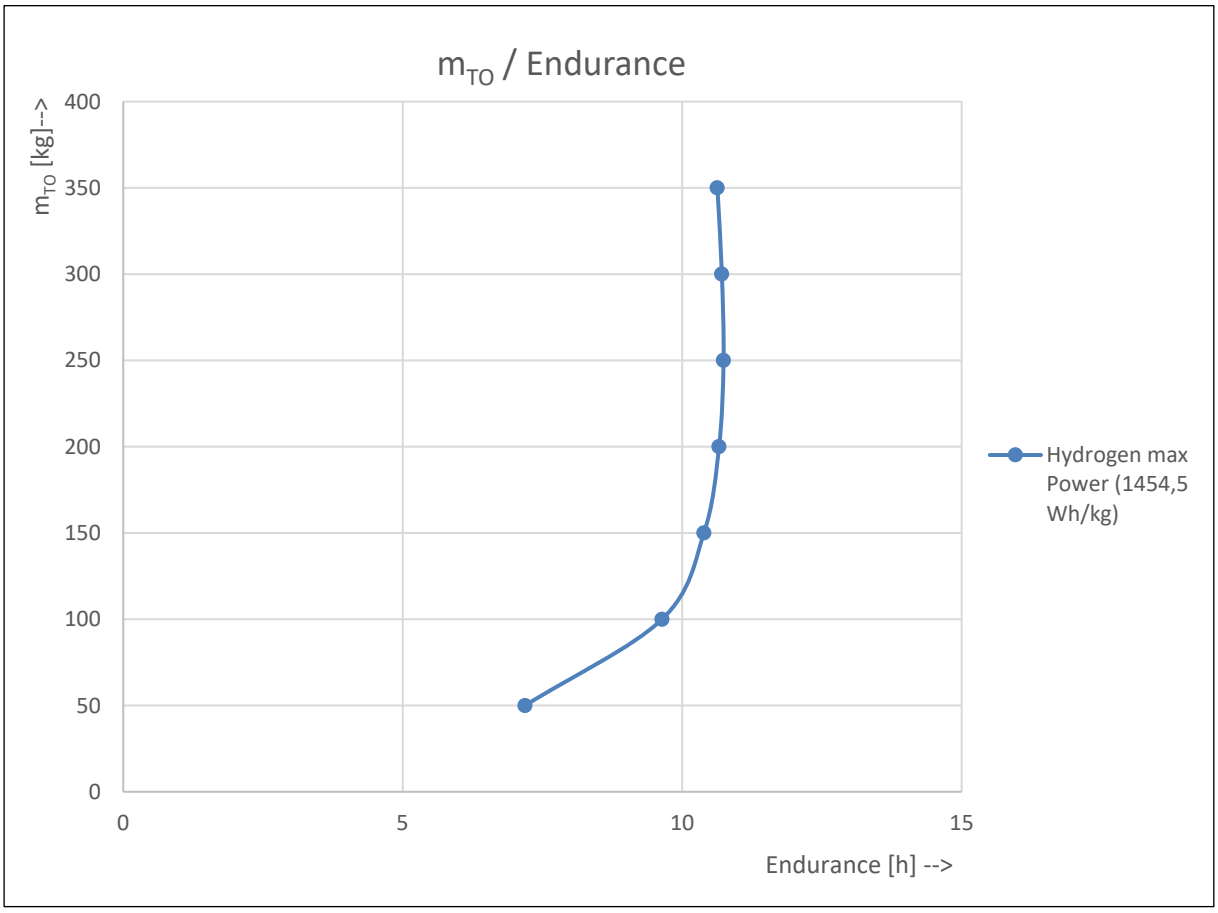

Figure 6.4 Take-off mass vs endurance of an example platform

In general, the take-off mass is made up of the payload mass m_{PL}, the fuel mass (here: battery mass m_B), and the empty mass m_E like equally described in Equation (2.2). Because the sum of the mass fractions must add up to 1, as shown in Equation (6.1), this is a constrain set for the evolutionary algorithm of Microsoft Excel to calculate the extreme value.

$$\frac{m_B}{m_{TO}} + \frac{m_E}{m_{TO}} + \frac{m_{PL}}{m_{TO}} = 1 \tag{6.1}$$

Table 6.3 Take-off masses of the design approaches

	Take-off mass m_{TO} [kg]	**Flight time $t_{m,Pmax}$ [h]**
Design 1	120,6	4,45
Design 2	119,66	4,41
Design 3	70,24	3,49

Table 6.3 shows the results of the take-off masses of the design approaches. Design 1 and 2 are optimized for maximum flight time, in consideration of the mass increase at maximum, shown in Figure 6.4, 0,5 hours are subtracted from the calculated maximum flight time. This reduced flight time is also given as flight time with maximum power $t_{m,Pmax}$ in Table 6.3.

Design 3 got an additional requirement of a maximum wingspan of 5 m and the take-off mass was calculated as described in Equation (6.2) with the wingspan b, the wing loading at the design point $\left(\frac{m}{S}\right)_{DP}$, and the wing aspect ratio AR.

$$m_{TO} = \frac{b^2 \cdot \left(\frac{m}{S}\right)_{DP}}{AR} \tag{6.2}$$

With

$$\begin{aligned} b &= 5\ \text{m} \\ \left(\frac{m}{S}\right)_{DP} &= 16{,}858\ \frac{\text{kg}}{\text{m}^2} \\ AR &= 6 \end{aligned}$$

Therefore

$$\begin{aligned} m_{TO} &= \frac{(5\ \text{m})^2 \cdot 16{,}858\ \frac{\text{kg}}{\text{m}^2}}{6} \\ m_{TO} &= 70{,}24\ \text{kg} \end{aligned}$$

6.3 Empty Mass

Equation (2.16) from Sadraey (2020, Sec. 2.8) shows an empirical solution to determine the empty mass fraction and is used analogous in this thesis.

$$\frac{m_E}{m_{TO}} = a \cdot m_{TO} + b \tag{6.3}$$

Equation (6.3) shows the analogue empirical solution to determine the empty mass fraction $\frac{m_E}{m_{TO}}$ with factors a and b, and dependent on the take-off mass m_{TO}.

To determine the factors a and b, an empirical study must be done. For this thesis, a small analysis of 31 motor glider was done. As basis motor glider where used, because the design idea was a drone with a high wing aspect ratio AR, and should be built lightweight.

Figure 6.5 shows data points of different motor gliders, lines of best fit and the corresponding linear equations created with the analysis. For further design the upper graph and therefore Equation (6.4) was used, because the fuel cells are considered to bring more weight than the commonly used propulsions. A table with the used database can be found in Appendix C.

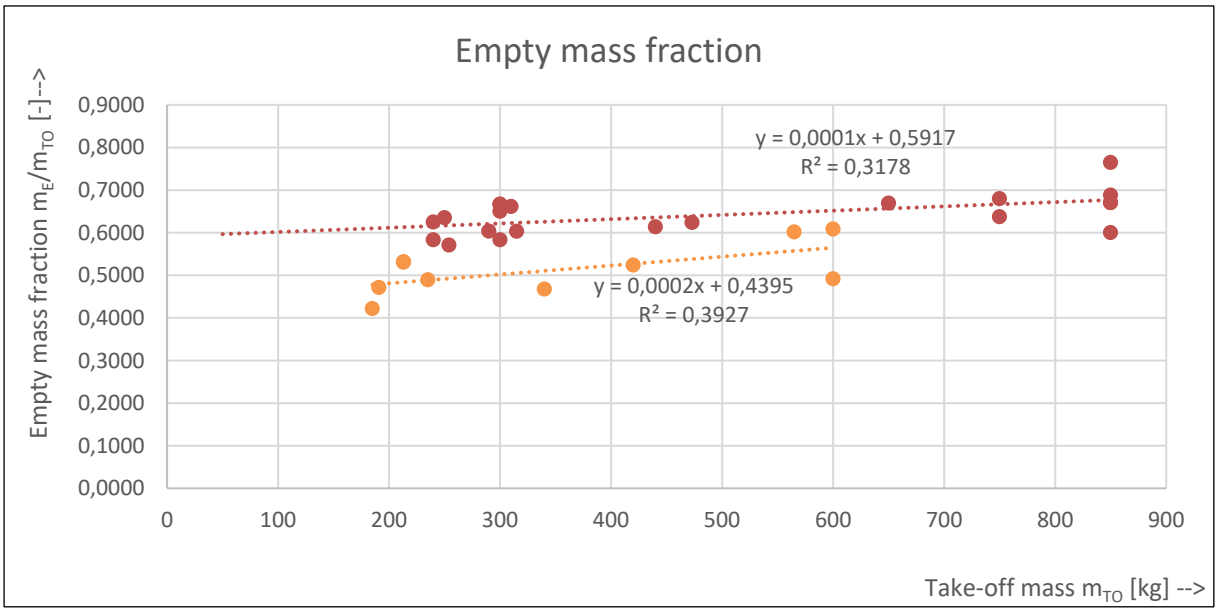

Figure 6.5 Empty mass fraction

$$\frac{m_E}{m_{TO}} = 0{,}0001 \cdot m_{TO} + 0{,}5917 \tag{6.4}$$

Equation (6.4) reveals the factor a with a value of 0,0001 and factor b with a value of 0,5917. It shows the value of the empty mass fraction changes with a change of the take-off mass.

With Equation (6.4) and the determined take-off masses m_{TO} from Section 6.2 the empty mass fractions (m_E/m_{TO}) and the empty masses m_E of the design approaches can be calculated, these are shown in Table 6.4.

Table 6.4 Empty masses of design approaches

	Take-off mass m_{TO} [kg]	Empty mass fraction $\frac{m_E}{m_{TO}}$ [-]	Empty mass m_E [kg]
Design 1	120,6	0,6038	72,82
Design 2	119,66	0,6037	72,24
Design 3	70,24	0,5988	42,06

6.4 Engine Power

The needed engine power is calculated analogous to Equation (2.31) as shown in Equation (6.5) with the determined take-off masses m_{TO} from Section 6.2, and the determined power-to-weight ratios $(P/m)_{DP}$ at the design points from Section 6.1. The results are shown in Table 6.5.

$$P_{Eng} = m_{TO} \cdot \left(\frac{P}{m}\right)_{DP} \tag{6.5}$$

Table 6.5 Engine power of the design approaches

	Take-off mass m_{TO} [kg]	Power-to-weight ratio $(P/m)_{DP}$ [W/kg]	Engine power P_{Eng} [W]
Design 1	120,6	100,31	12098
Design 2	119,66	101,05	12092
Design 3	70,24	104,37	7331

6.5 Fuel Mass

The fuel mass is mainly depending on the flight time and the power that needs to be supplied. In this thesis the fuel mass also includes the mass of the cylinders in which the hydrogen is stored. Therefore, the mass of the fuel is considered to be a during flight unchanged battery mass m_B, because the mass of the hydrogen is negligibly compared to the mass of the cylinders and will be referred as battery mass from now on. The needed power consists of the power used by the engines, and the power used by the systems and payload.

The flight time is a value that is calculated during the optimization process of the take-off mass. The needed power of the systems and payload P_{Sys} can be calculated from the systems that are considered to be used. These systems can be found in Section 3.3 and 3.4. The power

needed by the engines P_{Eng} is calculated in Section 6.4. Combined a total power P_{total} is calculated as shown in Equation (6.6).

$$P_{total} = P_{Sys} + P_{Eng} \tag{6.6}$$

The battery mass furthermore depends on the energy density E_D mentioned in Equation (2.14). To calculate the energy density of the hydrogen cylinders the specifications given in Table 3.7 and Equation (6.7) are used.

To get a design with a low as possible mass, the cylinder with the model's name A12 is used, due to its high specific energy of 10.471 kJ/kg. Given are the electrical energy E stored with the hydrogen as 4800 Wh at an estimate of 50% efficiency and the mass of the cylinder m_C with 3,3 kg.

$$E_D = \frac{Energy}{mass}$$
$$E_D = \frac{E}{m_C} \tag{6.7}$$

With

$$E = 4800 \text{ Wh}$$
$$m_C = 3{,}3 \text{ kg}$$

Therefore

$$E_D = \frac{4800 \text{ Wh}}{3{,}3 \text{ kg}}$$
$$E_D = 1454{,}55 \frac{\text{Wh}}{\text{kg}}$$

The battery mass m_B is calculated with the flight time t_m, calculated in the optimization of the take-off mass, the total Power needed P_{total}, and the energy density E_D. This calculation is shown in Equation (6.8), which is equal to Equation (2.15), and the results for the design approaches are shown in Table 6.6.

$$m_B = \frac{t_m \cdot P_{total}}{E_D} \tag{6.8}$$

Table 6.6 Battery mass of the design approaches

	Flight time $t_{m,Pmax}$ [h]	**Total power P_{total} [W]**	**Energy density E_D [Wh/kg]**	**Battery mass m_B [kg]**
Design 1	4,45	12348	1454,55	37,78
Design 2	4,41	12342	1454,55	37,42
Design 3	3,49	7581	1454,55	18,19

6.6 Wing Area and Wingspan

To calculate the wing area, Equation (6.9) is used analogous to Equation (2.4) with the determined take-off masses from Section 6.2, and the wing loadings $(m/S)_{DP}$ at the design points from Section 6.1. The results are shown in Table 6.7.

$$S_W = m_{TO} / \left(\frac{m}{S}\right)_{DP} \tag{6.9}$$

Table 6.7 Wing area of the design approaches

	Take-off mass m_{TO} [kg]	**Wing loading $(m/S)_{DP}$ [kg/m²]**	**Wing area S_W [m²]**	**Wingspan b [m]**
Design 1	120,6	16,858	7,16	11,97
Design 2	119,66	16,858	7,1	9,97
Design 3	70,24	16,858	4,17	5,00

To calculate the wingspan, the values of Table 6.1, the previous calculated wing areas from Table 6.7, and the Equation (6.11), converted from Equation (2.5), are used as shown below.

$$b = \sqrt{A \cdot S} \tag{6.10}$$

With

$$A = AR$$
$$S = S_W$$

Therefore

$$b = \sqrt{AR \cdot S_W} \tag{6.11}$$

Equation (6.11) calculates the wingspan b with the aspect ratio of the wing AR and the wing area S_W. The results are shown in Table 6.7.

6.7 Maximum Mission Time and Range

The drone will not be operating with the maximum speed $V_{\max}$ the whole time, so the needed power for the cruise and loiter must be determined.

The calculation of the power in cruise P_C is analogous to the calculation of the maximum power. This is shown in Equation (6.12) and (6.13).

$$\left(\frac{P_{SL}}{m}\right)_{V_C} = \left(\frac{P_{SL}}{W}\right)_{V_C} \cdot g = \frac{\frac{1}{2}\rho_0 V_C^3 C_{D_0} \frac{1}{\left(\frac{W}{S}\right)} + \frac{2K}{\rho\sigma V_C}\left(\frac{W}{S}\right)}{\eta_P} \cdot g \tag{6.12}$$

With

$$\rho_0 = 1{,}225\ \frac{\mathrm{kg}}{\mathrm{m}^3}$$
$$\rho = \rho_C = 1{,}167\ \frac{\mathrm{kg}}{\mathrm{m}^3}$$
$$\sigma = 0{,}9529$$
$$g = 9{,}81\ \frac{\mathrm{m}}{\mathrm{s}^2}$$

Therefore

$$\left(\frac{W}{S}\right) = \left(\frac{W}{S}\right)_d = \left(\frac{m}{S}\right)_{DP} \cdot g = 165{,}375\ \frac{\mathrm{N}}{\mathrm{m}^2}$$

$$P_C = \left(\frac{P_{SL}}{m}\right)_{V_C} \cdot m_{TO} \tag{6.13}$$

For the calculation of the maximum mission time with cruise power $t_{m,c}$, equivalent to Equation (2.14), Equation (6.14), with the power in cruise P_C, the system power P_{Sys}, the battery mass m_B, and the energy density of the battery E_D, is used.

$$t_{m,c} = \frac{m_B \cdot E_D}{P_C + P_{sys}} \tag{6.14}$$

The range R is calculated without climb or descent with Equation (6.15).

$$R = V_C \cdot t_{m,c} \tag{6.15}$$

The results of the calculations with the values of Table 6.1 and Section 6.1 are shown in Table 6.8.

Table 6.8 Mission time and range of the design approaches

	Power-to-weight ratio in cruise $(P/m)_{V_C}$ [W/kg]	**Power in cruise P_C [W]**	**Maximum mission time $t_{m,c}$ [h]**	**Range R [km]**
Design 1	31,82	3837	13,44	1344
Design 2	32,93	3941	12,98	1298
Design 3	37,91	2663	9,08	908

6.8 Evaluation of Designs

6.8.1 Evaluation Criteria

To evaluate design options, the following criteria were considered:

1. Weight
2. Range
3. Endurance
4. Speed
5. Size
6. Ground service
    a. Turn around time
    b. Parking and storage
7. Redundancy
    a. Engine
    b. Power supply

The following criteria were assumed as K.O.-criteria:

1. Maximum take-off mass greater than 400 kg
2. Cruise speed less than 100 km/h
3. Stall speed greater than 25 m/s

6.8.2 Evaluation Matrix

Table 6.9 Evaluation matrix

			Design 1		Design 2		Design 3	
		Weighting factor (Sum is 1)	*Rating (1-5)*	*Weighted rating*	*Rating (1-5)*	*Weighted rating*	*Rating (1-5)*	*Weighted rating*
Criteria	Take-off mass	0,13	3	0,39	3	0,39	4	0,52
	Range	0,22	3	0,66	2	0,44	1	0,22
	Endurance	0,22	3	0,66	3	0,66	2	0,44
	Speed	0,17	3	0,51	3	0,51	3	0,51
	Size	0,09	3	0,27	4	0,36	5	0,45
	Ground service	0,13	2	0,26	3	0,39	5	0,65
	Redundancy	0,04	5	0,2	5	0,2	5	0,2
	Sum	1		**2,95**		**2,95**		**2,99**

Table 6.9 shows the evaluation matrix generated for three design options. The criteria are weighted, and every design option is given points, from 1 point which means the design underperforms in this criterion to 5 points which means the design performs well in this criterion. At the bottom line, the weighted rating of every design option is added, and the best option can be chosen by selecting the one with the highest sum of weighted rating.

With these minor differences in design, it is no wonder, that the ratings are remarkably close, but design 3 is rated the highest and the values of this design approach will be used for further calculations and design.

7 Fuselage Design

To determine the dimensions of the drone, drafts of the cross sections of the fuselage were made. In the draft of the cross sections of the yz-plane in Figure 7.1 the stack of hydrogen cylinders, the stack of fuel cells and the camera can be seen. In the draft of the cross section of the xz-plane in Figure 7.2 the relative position of the radar, the avionics, the fuel cell stacks, the hydrogen cylinder stack, the camera, and the GPS antennas on the x-axis can be seen.

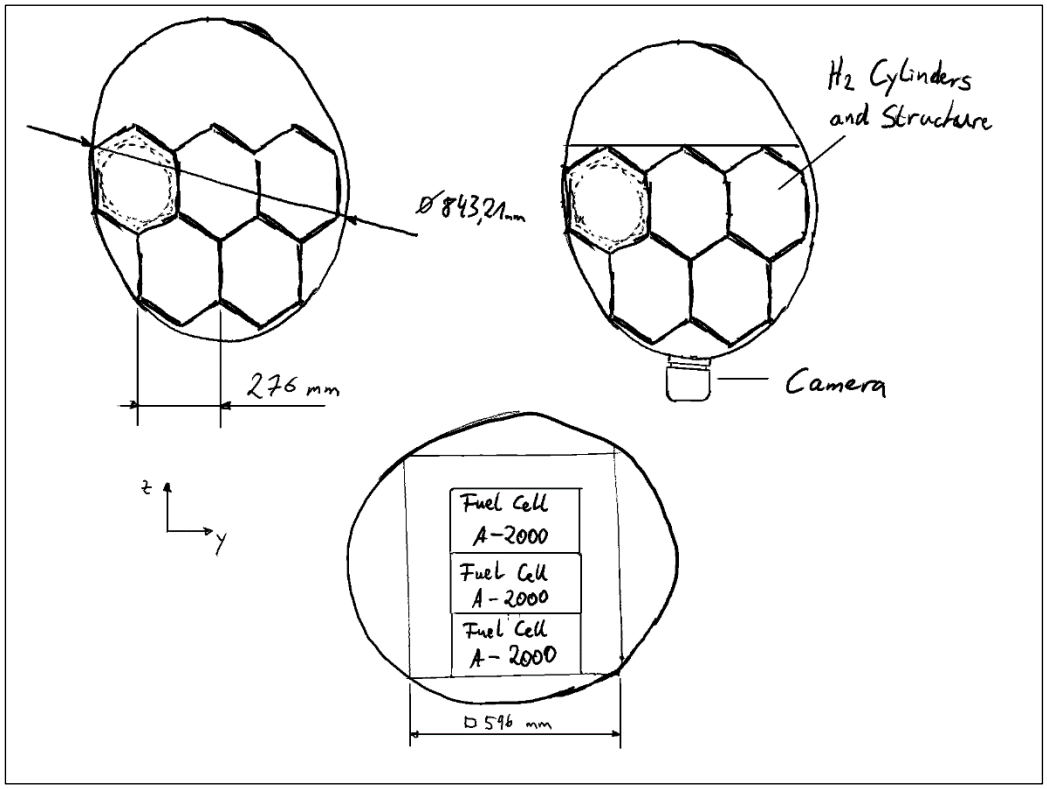

Figure 7.1 Cross section of yz-plane of the design approach

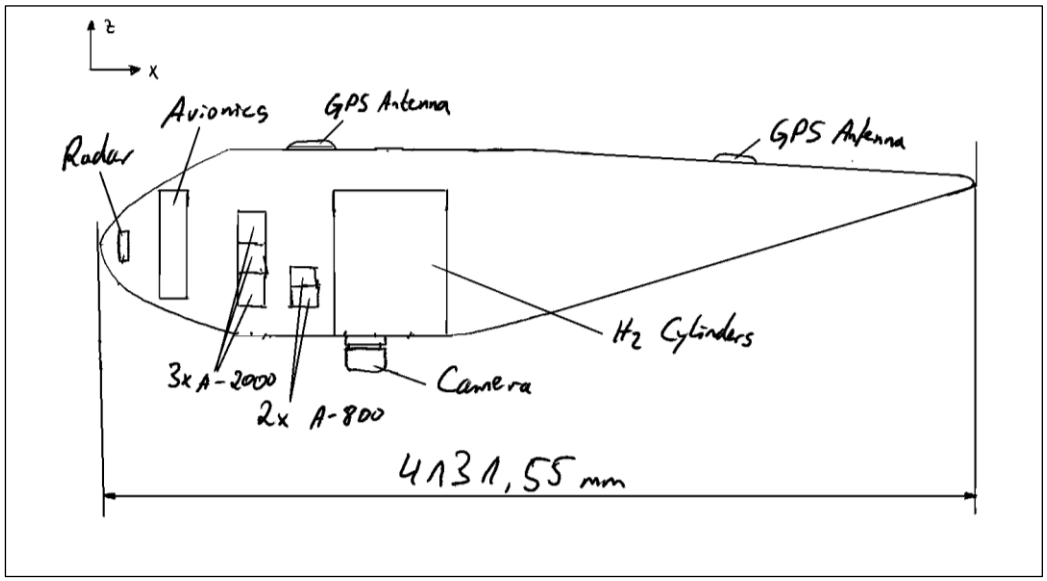

Figure 7.2 Cross section of xz-plane of the design approach

8 Conceptual Design

8.1 Mass Distribution and Center of Gravity

To assume the position of the center of gravity (CG) and the mass distribution of the drone, the drafts of the fuselage of Chapter 7, the weights given in Tables 3.1 through 3.7, and the weights and values determined in Chapter 6 are taken as a basis.

Weights of the fuselage, wings, and tailplane are not calculated yet. The assumption of these weights will be made with the empirically determined weight fractions by Roskam (2018b, Appendix A, Table 1.1b). To compensate the different empty weight ratios of the aircraft used by Roskam and the design approach of this thesis, the weight fractions of the structure are calculated with Equation (8.1). These weight fractions are shown in Table 8.1.

$$f_{S,i} = \frac{f_{GW,i}}{\sum f_{GW,i}} \tag{8.1}$$

Table 8.1 Weight fractions of components for homebuilt propeller driven airplanes (modified from Roskam 2018b, Table A1.1b)

	Weight fraction of GW [-]	Weight fraction of structure [-]
Wing group	0,083	0,451
Empenn. group	0,016	0,087
Fuselage group	0,085	0,462

The structural mass of the drone m_S is calculated with Equation (8.2).

$$m_S = m_E - m_{Avionics} - m_{Engines} - m_{Power\ Supply} \tag{8.2}$$

With the weight fractions of Table 8.1 and the determined, with Equation (8.2), structural mass of 24,97 kg, the wing group will have a mass of 11,26 kg, the empennage group will have a mass of 2,17 kg, and the fuselage group will have a mass of 11,54 kg.

Another still missing weight is the one of the engines. The assumption here is that an electric engine has a power-to-weight ratio of 5000 W/kg. This power-to-weight ratio is given by Siemens (2015) for an electric motor for aircraft. With this power-to-weight ratio and the calculated engine power of 7331 W from Table 6.6 the two engines will have a mass of 0,7331 kg each.

To supply the needed electrical power stated in Section 6.5, the fuel cells need to provide a total of 7581 W. With three A-2000 and two A-800 fuel cells a total of 7600 W can be provided. The mass of the three A-2000 is 9 kg, and the mass of the two A-800 is 2,46 kg.

The assumed distribution of the mass groups of the drone is shown in Figure 8.1 and Table 8.2.

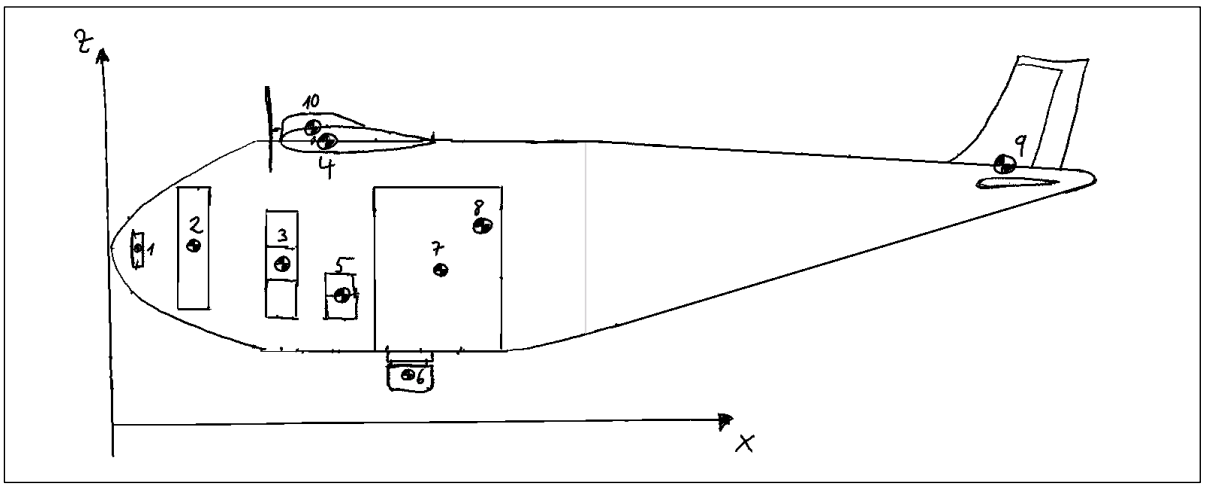

Figure 8.1 Assumed mass distribution of the design approach – side view

Table 8.2 Assumed values of mass distribution of the design approach

#	Mass Group	Mass [kg]	x-position [mm]	$m_i \cdot x_i$ [kg · mm]	z-position [mm]	$m_i \cdot z_i$ [kg · mm]
1	Radar	0,7	140	98	725	507,5
2	Avionics	3,454	377	1302,158	725	2504,15
3	3x A-2000	9	740	6660	646	5814
4	Wing group	11,26	949	10685,74	1133	12757,58
5	2x A-800	2,46	977	2403,42	527	1296,42
6	Camera	6,8	1256	8540,8	211	1434,8
7	5x hydrogen cylinders	18,19	1396	25393,24	619	11259,61
8	Fuselage group	11,54	1591	18360,14	791	9128,14
9	Empennage group	2,17	3741	8117,97	1015	2202,55
10	2x engines	1,47	893	1312,71	1186	1743,42
Sum		67,044	**1236,12**	82874,178	**725,62**	48648,17

Table 8.2 shows the mass groups, their masses, the x-positions of the individual centers of gravity, and the products of the mass and x-position. The masses of the mass groups were determined in Sections 3.3 through 3.5, Section 6.5, and this Section above. The shown sum is the sum of all mass groups, the sum of the x-positions is the calculated x-position of the overall center of gravity and has the value 1236,12 mm. The x-position of the overall center of gravity was calculated with the Equation (2.6). The z-position of the overall center of gravity was calculated analogous to the x-position and has a value of 725,62 mm.

8.2 Neutral Point and Dimension of the Wings

As stated in Section 6.6, the wing area of the chosen design approach is 4,17 m^2 and the wingspan 5 m. To achieve a near elliptical lift distribution and therefore less induced drag a tapered wing can be considered. In this thesis the wing is not tapered and therefore a rectangular wing. Also, for this approach a symmetrical profile is chosen, and the wing has therefore no pitching momentum.

Table 8.3 Dimensions of the wing

Wingspan:	5,00 m
Wing area:	4,17 m^2
Chord length:	0,834 m

$$c = \frac{S}{b} \tag{8.3}$$

Equation (8.3) is used to calculate the chord length of the wing c with the given wing area S and the given wingspan b. All calculated and defined values of the wing's dimensions can be seen in Table 8.3.

8.3 Size and Position of the Empennage

8.3.1 Horizontal Tailplane

For the calculation of the needed horizontal tailplane, Equation (2.7) is used and the momentum around the center of gravity M_{CG} must be 0. The center of gravity, the aerodynamic centers and applied forces like Thrust T, lift of the wings L_W, and lift of the vertical tailplane L_V are shown in Figure 8.2. The levers to the center of gravity, the values of these forces, and the resulting momenta around the center of gravity are listed in Table 8.4. The aerodynamic centers are assumed to be at 1/4 of the mean aerodynamic chord of the profiles.

$$T = \frac{P \cdot \eta_P}{V} \tag{8.4}$$

$$L = \frac{1}{2} C_L \cdot \rho \cdot V^2 \cdot S \tag{8.5}$$

$$\Leftrightarrow S = \frac{2L}{C_L \cdot \rho \cdot V^2}$$

Equation (8.4) calculates the thrust T produced by a propeller engine with the power P, the propeller efficiency η_P, and the speed V. Equation (8.5) calculates the lift L with the lift coefficient C_L, the air density ρ, the speed V, and the wing area S.

As the critical state for sizing the horizontal tailplane, the take-off was identified. For that reason, the values for take-off are used.

Table 8.4 Forces in xz-plane and momenta around y-axis

Force	Value of force [N]	Lever [mm]	Momentum around CG [Nmm]
Take-off thrust $\boldsymbol{T_{TO}}$	-355,44	474	-168478,56
Lift of the wing $\boldsymbol{L_W}$	834,43	461	384672,23
Lift of the vertical tailplane $\boldsymbol{L_H}$	94,86	2279	-216193,67

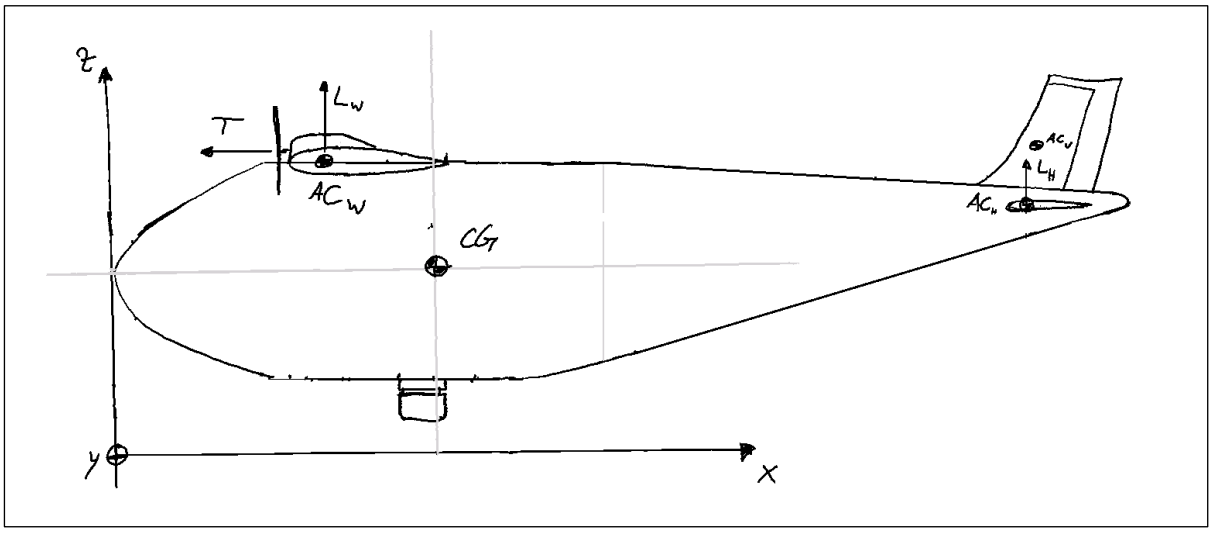

Figure 8.2 Location of forces and center of gravity − side view

With Equation (8.5), the calculated lift from Table 8.4, an assumed lift coefficient of the horizontal tailplane of 0,5, the air density, and the take-off speed, the needed area of the horizontal tailplane S_H is calculated.

$$S_H = 1{,}14\ \mathrm{m}^2$$

8.3.2 Vertical Tailplane

The needed area of the vertical tailplane is calculated with Equation (2.8) through (2.13), determined values of Figures 2.1 and 2.2, the location of the forces, aerodynamic center of the vertical tailplane, and center of gravity from Figure 8.3, and the assumed values below. The aerodynamic center is assumed to be at 1/4 of the mean aerodynamic chord of the profile.

Equation (2.8) with

$$V_S = 15\ \frac{\mathrm{m}}{\mathrm{s}}$$
$$T_{TO} = 355{,}44\ \mathrm{N}$$
$$n_E = 2$$
$$y_E = 0{,}834\ \mathrm{m}$$
$$\delta_F = 20° \triangleq \frac{1}{9}\pi$$
$$c_f/c = 0{,}3$$
$$t/c = 0{,}15$$
$$(c_{L,\delta})_{theroy} = 4{,}6$$
$$\frac{c_{L,\alpha}}{(c_{L,\alpha})_{theory}} = 0{,}8$$
$$\frac{c_{L,\delta}}{(c_{L,\delta})_{theory}} = 0{,}68$$
$$K' = 0{,}79$$
$$\varphi_{25} = 5° \triangleq \frac{1}{36}\pi$$
$$l_V = 2{,}397\ \mathrm{m}$$

Therefore

$$S_V = 2{,}16\ \mathrm{m}^2$$

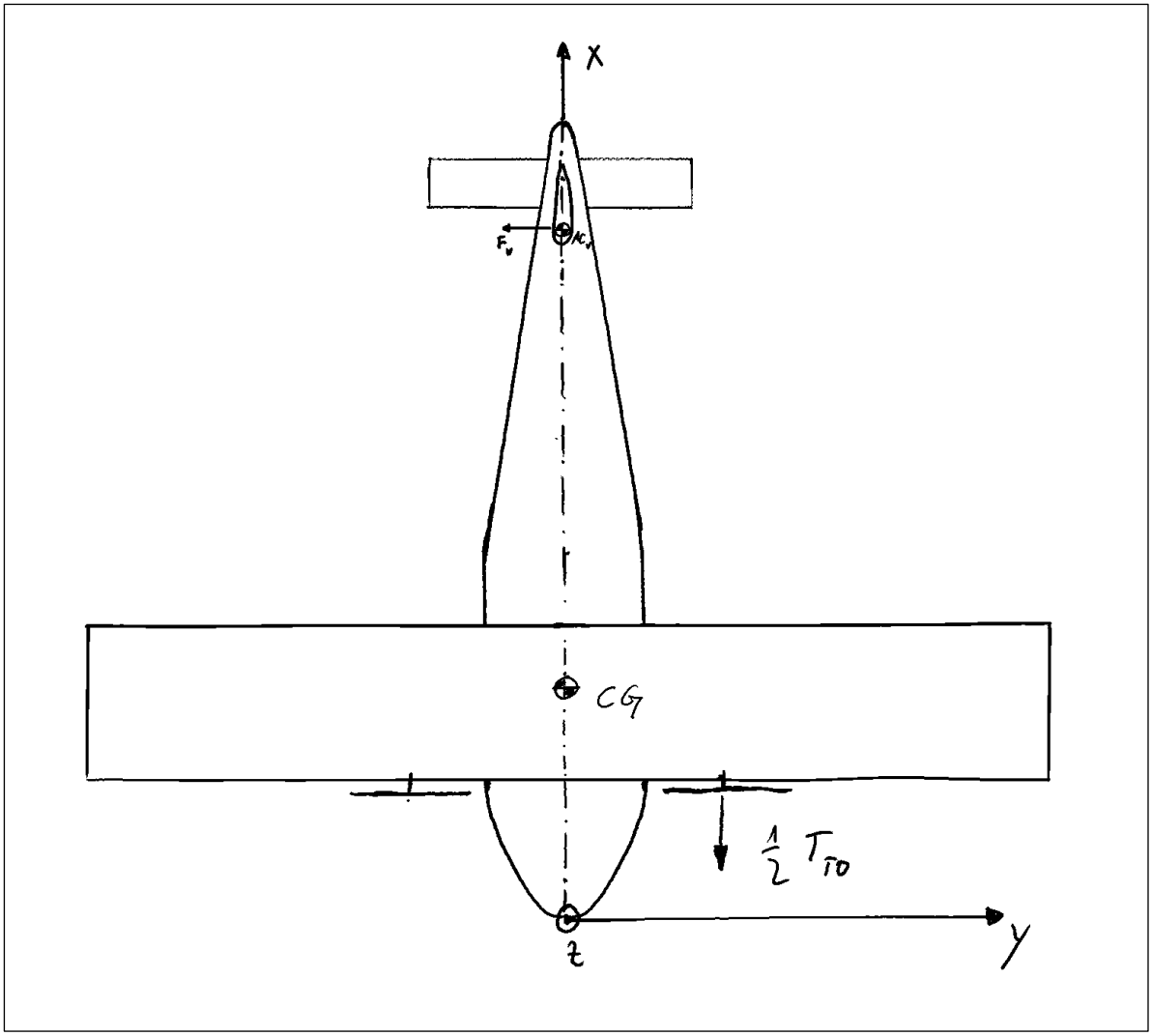

Figure 8.3 Location of forces and center of gravity – top view

9 Summary

The most important requirement was defined as the hydrogen fuel cell propulsion system in Section 3.2. To meet this requirement led to sacrifice of other requirements in the process. An operating time of 24 to 30 hours, and a range of 2400 to 3600 km were demanded, but the chosen design approach only achieves a flight time of 9 hours, and a range of 900 km. The requirements of the payload mass and wingspan are met, but the aspect ratio needed to be adjusted to one that cannot be considered as high aspect ratio. The demanded maximum speed was not reached due to severe increase of needed engine power. The demanded rate of climb could even be approved from 300 m/min to 650 m/min, like described below.

In Section 6.1 the matching charts of the different design approaches were made. In all matching charts it can be seen that only the maximum speed is decisive. This leads to the insight, that the assumed performance parameters of the take-off run, climb and at absolute ceiling can be improved. Figure 9.1 shows a new matching chart with adjusted performance parameters shown in Table 9.1. The calculations were done analogously to Section 6.1.

Table 9.1 Adjusted performance parameters for Design 3

Input variables	
Maximum speed $V_{\max}$ [km/h]	150
Cruise speed V_C [km/h]	100
Stall speed V_S [km/h]	54
Take-off distance S_{TO} [m]	**50**
Rate of climb ROC [m/min]	**650**
Cruise altitude [m]	500
Absolute ceiling h_C [m]	**10300**
Wing aspect ratio AR [-]	6
Payload mass m_{PL} [kg]	10
Oswald factor e [-]	0,8
Max lift coefficient $C_{L_{\max}}$ [-]	1,2
Lift-to-drag ratio L/D [-]	12
Zero-lift drag coefficient C_{D_0} [-]	0,03
Propeller efficiency η_P [-]	0,8
Friction coefficient landing strip μ [-]	0,04
System power consumption P_{Sys} [W]	250

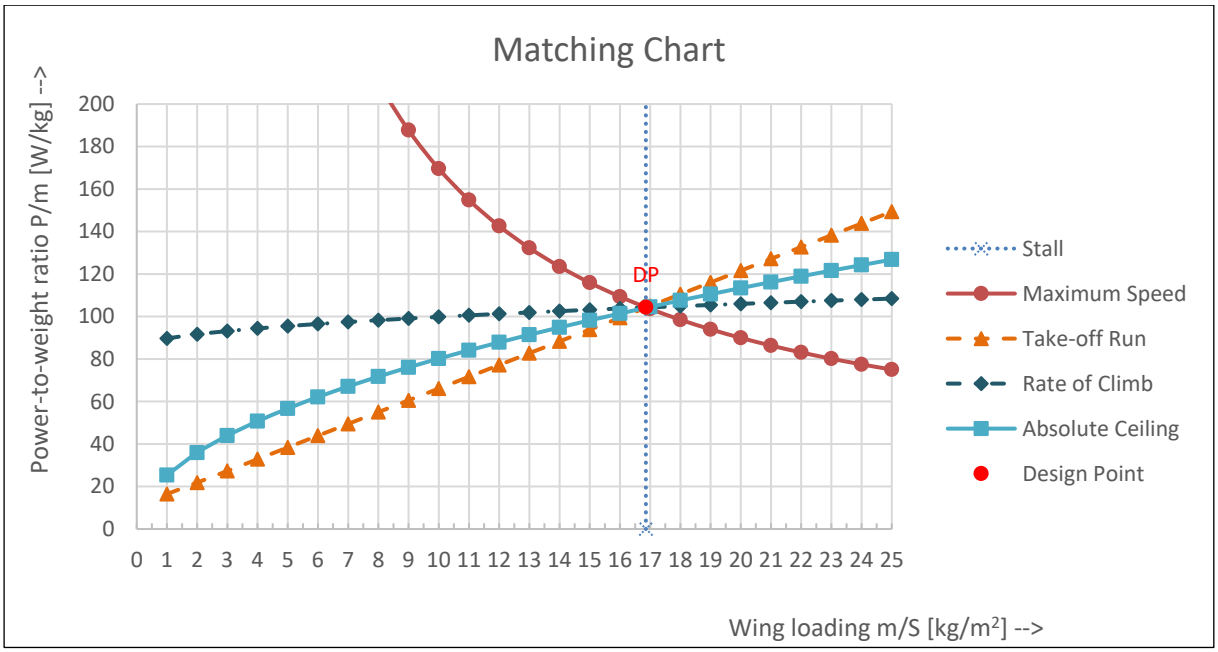

Figure 9.1 Matching chart of Design 3 with adjusted performance parameters

Figure 9.1 and Table 9.1 show an improvement of the take-off distance from 80 m to 50 m, rate of climb from 300 m/min to 650 m/min, and absolute ceiling from 4.000 m to 10.300 m, without changing the wing loading or the power-to-weight ratio.

In Section 6.5 it became clear that even with a high aspect ratio and a high lift-to-drag ratio, the flight time of a hydrogen powered drone is very limited. In those scales due to the limited energy density of the hydrogen linked with the quite heavy gas cylinders, and the heavy fuel cells, the requirements of flight time and range cannot be met. To be regarded is also that in Section 6.1 a fixed propeller efficiency is used, and this is due to the model building of the calculation, but the effect of lower propeller efficiency while take-off and landing must be kept in mind later.

In Section 8.3.2 the area of the vertical tailplane was calculated. Noticeable is that the vertical tailplane needs to be very large, because of the great power of the engines needed. The engine size is caused by the maximum speed requirement, all other performance parameters were not decisive at that state of the design.

A summary of the most important performance and dimension parameters, and the considered systems is given in Table 9.2.

Table 9.2 Overview of dimensions and performance of the final design

Wing:	**Braced rectangular high wing**
Area:	4,17 m^2
Aspect ratio:	6
Wingspan:	5,00 m
Empennage:	**Conventional tail**
Horizontal area:	1,14 m^2
Vertical area:	2,16 m^2
Fuselage:	
Length:	4,14 m
Diameter:	0,844 m
Engines:	**2x electrical**
Total power:	7331 W
Fuel Cells:	**3x A-2000, 2x A-800**
Total provided power:	7600 W
Total consumption:	79,6 l/min
Payload:	**Wescam MX-8 camera**
Weight:	6,8 kg
MTOW:	**70,24 kg**
Performance:	
Max. speed:	150 km/h
Cruise speed:	100 km/h
Stall speed:	54 km/h
Take-off distance:	50 m
Rate of climb:	650 m/min
Cruise altitude:	500 m
Absolute ceiling	10.500 m

10 Conclusions and Recommendations

The definition of the cruise altitude in Section 3.2 is difficult and leads to problems with the calculation. A fixed cruise altitude needs to be defined for calculations, but in the case of a wildfire detection drone, this cruise altitude, contrary to passenger aircraft, is varying at various locations with different ground elevations. To meet the changing requirements of different operation locations a design with changeable wings could be considered when carrying this project forward.

The design approach in this thesis is not only based on the methods used in conventional aircraft design, as planned in the beginning. The reason for that deviation from the known methods and the usage of calculations for drones is, that for the methods of conventional aircraft design, assumptions on empirically obtained factors need to be done. The knowledge about those factors is not existing to this moment and a future study to determine those factors would be meaningful.

The acquired drone design does not meet all requirements due to lack of experience with hydrogen powered aircraft. To avoid the assumption of too high expected requirements, an empirically build knowledge must be gained. This knowledge also can help with the decision making on assumed parameters like the lift-to-drag ratio, the Oswald factor, and the stall speed. For a design of a hydrogen powered aircraft with fuel cells, the higher weight of the components and the fuel storage must be kept in mind, because with a fuel like hydrogen, that even has a higher energy density than gas or jet fuel, the weight of the gas cylinders must be taken into account. The weight of the gas cylinders declines the overall energy density because the gas cylinders cannot be implemented in the structure like a conventional fuel tank with more than one purpose in the means of the lightweight construction philosophy.

A drone with the demanded requirements is by all means not reasonable, because of the high wanted maximum speed. An aircraft design with more wingspan, therefore a much higher take-off mass, in combination of a greater stall speed and a high lift system would be feasible to reach those goals.

For further construction of the designed drone, a CAD model must be made to analyze the used space for all integrated systems and payload, to verify the calculations on center of gravity and the empennage sizing, and to do a stability and fluid flow analysis. For further analysis of the drone, the wing profile and the propeller must be chosen. A future implementation for a calculation of the different propeller efficiencies at the different performances will be useful to eliminate the assumption of a fixed propeller efficiency. A stability analysis for the empennage sizing is pending with a change of the payload and payload mass as the possibility of interchangeable payloads should be considered. To optimize the design the wing parameters can be analyzed and adjusted.

List of References

BRITANNICA DICTIONARY, 2023. *Detection*.
Available from: https://www.britannica.com/dictionary/detection
Archived at: https://perma.cc/DK36-QZ4Q

BUSINESS INSIDER, 2023. *The Black Swan*.
Available from: https://bit.ly/47pPGYi
Archived at: https://perma.cc/H2VY-WXLZ

CAMBRIDGE DICTIONARY, 2023a. *Design*.
Available from: https://dictionary.cambridge.org/de/worterbuch/englisch/design
Archived at: https://perma.cc/4BQ8-2GAR

CAMBRIDGE DICTIONARY, 2023b. *Requirement*.
Available from: https://bit.ly/3R5VyPR
Archived at: https://perma.cc/887M-Z5H4

CAT UAV, 2023. *ORYX*.
Available from: https://bit.ly/49BnQdk
Archived at: https://perma.cc/5RPN-PQTX

COLLINS DICTIONARY, 2023a. *Hydrogen*.
Available from: https://www.collinsdictionary.com/de/worterbuch/englisch/hydrogen
Archived at: https://perma.cc/6YHW-G62C

COLLINS DICTIONARY, 2023b. *Powered*.
Available from: https://www.collinsdictionary.com/de/worterbuch/englisch/powered
Archived at: https://perma.cc/UMK2-DJ6F

COLLINS DICTIONARY, 2023c. *Empennage*.
Available from: https://www.collinsdictionary.com/de/worterbuch/englisch/empennage
Archived at: https://perma.cc/UBL7-DCJW

COLLINS DICTIONARY, 2023d. *Gas Cylinder*.
Available from: https://www.collinsdictionary.com/de/worterbuch/englisch/cylinder
Archived at: https://perma.cc/75W2-SJP6

COLLINS DICTIONARY, 2023e. *Patrol*.
Available from: https://www.collinsdictionary.com/de/worterbuch/englisch/patrol
Archived at: https://perma.cc/3JUL-AM8C

DBPEDIA, 2023. *Loiter*.
Available from: https://dbpedia.org/page/Loiter_(aeronautics)
Archived at: https://perma.cc/JH2R-QNGQ

DRONAMICS, 2023. *The Black Swan*.
Available from: https://www.dronamics.com/theblackswan
Archived at: https://perma.cc/F6E7-7UFF

EMBENTION, 2023. *Veronte Autopilot 4x*.
Available from: https://www.embention.com/product/veronte-autopilot-4x/
Archived at: https://perma.cc/SH24-ER93

ENCYCLOPEDIA BRITANNICA, 2023a. *Disaster*.
Available from: https://www.britannica.com/science/disaster
Archived at: https://perma.cc/2HXF-85G5

ENCYCLOPEDIA BRITANNICA, 2023b. *Greenhouse Gas*.
Available from: https://www.britannica.com/science/greenhouse-gas
Archived at: https://perma.cc/GJJ9-ML2M

FCHEA, 2023. *Fuel Cells*.
Available from: https://www.fchea.org/fuelcells
Archived at: https://perma.cc/7YBG-D56K

GUDMUNDSSON, Snorri, 2014. *General Aviation Aircraft Design: Applied Methods and Procedures*. Oxford, UK: Elsevier Inc.
Available from: https://doi.org/10.1016/C2011-0-06824-2 (Closed Access)

H3 DYNAMICS, 2023. *Unmanned Aviation Brochure*.
Available from: https://bit.ly/3GqxK45
Archived at: https://perma.cc/V8T4-U2TV

HONEYWELL, 2023. *IntuVue RDR-84K*.
Available from: https://bit.ly/47RRxVW
Archived at: https://perma.cc/C2Y4-LC93

IRIS AUTOMATION, 2023. *Casia X*.
Available from: https://www.irisonboard.com/casia/
Archived at: https://perma.cc/E5B4-FR5V

MAPFRE, 2023. *Environmental Impact*.
Available from: https://bit.ly/3NaLuUy
Archived at: https://perma.cc/375F-7KSM

MERRIAM WEBSTER, 2023a. *Configuration*.
Available from: https://www.merriam-webster.com/dictionary/configuration
Archived at: https://perma.cc/MF8D-3XHY

MERRIAM WEBSTER, 2023b. *Payload*.
Available from: https://www.merriam-webster.com/dictionary/payload
Archived at: https://perma.cc/H9MF-BZY2

MERRIAM WEBSTER, 2023c. *Performance*.
Available from: https://www.merriam-webster.com/dictionary/performance
Archived at: https://perma.cc/4SEN-83Q3

MERRIAM WEBSTER, 2023d. *Tailplane*.
Available from: https://www.merriam-webster.com/dictionary/tailplane
Archived at: https://perma.cc/A23Q-9SNT

NATIONAL GEOGRAPHIC, 2023. *Wildfires*.
Available from: https://education.nationalgeographic.org/resource/wildfires/
Archived at: https://perma.cc/9RLN-WNAG

NOAA, 2023. *LiDAR*.
Available from: https://oceanservice.noaa.gov/facts/lidar.html
Archived at: https://perma.cc/N6M3-8YES

NORTHWEST UAV, 2023. *PING-200SR*.
Available from: https://bit.ly/3Gkzufh
Archived at: https://perma.cc/2NS3-5R6F

PRIMOCO, 2023. *Primoco UAV One 150*.
Available from: https://uav-stol.com/primoco-uav-one-150/
Archived at: https://perma.cc/H58C-DBKW

ROSKAM, Jan, 1985. *Airplane Design*. Part 1: *Preliminary Sizing of Airplanes*. Ottawa, Kansas, USA: Roskam Aviation and Engineering Corporation

ROSKAM, Jan, 2018a. *Airplane Design*. Part 2: *Preliminary Configuration Design and Integration of the Propulsion System*. Lawrence, Kansas, USA: DARcorporation

ROSKAM, Jan, 2018b. *Airplane Design*. Part 5: *Component Weight Estimation*. Lawrence, Kansas, USA: DARcorporation

SADRAEY, Mohammad H., 2020. *Design of Unmanned Aerial Systems*. Southern New Hampshire University. Manchester, NH, USA: John Wiley & Sons Ltd
Available from: https://doi.org/10.1002/9781119508618 (Closed Access)

SCHOLZ, Dieter, 2015. *Aircraft Design*. Lecture Notes. Hamburg University of Applied Science, Department of Automotive and Aeronautical Engineering
Available from: http://lecturenotes.aircraftdesign.org/

SIEMENS, 2015. *Elektromotor für Luftfahrzeuge*.
Available from: https://bit.ly/412kRqA
Archived at: https://perma.cc/334D-8TAS

SKY DRONE, 2023. Sky Drone Link 3.
Available from: https://bit.ly/3QYSdlK
Archived at: https://perma.cc/3Z5G-N3YC

SKYETON, 2023. *Raybird 3*.
Available from: https://skyeton.com/en/raybird/
Archived at: https://perma.cc/KA23-UREL

TELEMETER, 2023. *MX-8*.
Available from: https://telemeter.info/de/mwdownloads/download/link/id/378
Archived at: https://perma.cc/4YK8-R76N

UST, 2023. *Long Endurance Drones*.
Available from: https://bit.ly/3EUv5iB
Archived at: https://perma.cc/Z5UN-YUCG

VOLATUS AEROSPACE, 2023. *Flexrotor*.
Available from: https://volatusaerospace.com/flexrotor/
Archived at: https://perma.cc/9QDZ-96H2

WIKIPEDIA, 2023. *Rotation*.
Available from: https://en.wikipedia.org/wiki/Rotation_(aeronautics)
Archived at: https://perma.cc/N6ZT-Z5BN

All online resources have been accessed on 2023-12-10 or later.

Appendix A – Extracts from Literature

Table A.1 Group weight data for homebuilt propeller driven airplanes (Roskam 2018b)

Table A1.1b Group Weight Data for Homebuilt Propeller Driven Airplanes

Type	Bede BD5B	At the time of printing no other data were available
Flight Design Gross Weight, GW, lbs	1,051	
Structure/GW	0.214	
Power Plant/GW	0.180	
Fixed Equipm't/GW	0.119	
Empty Weight/GW	0.513	
Wing Group/GW	0.083	
Empenn. Group/GW	0.016	
Fuselage Group/GW	0.085	
Nacelle Group/GW	0.000	
Land. Gear Group/GW	0.030	
Take-off Gross Wht, W_{TO}, lbs	1,051	
Empty Weight, W_E, lbs	539	
Wing Group/S, psf	1.8	
Emp. Grp/S_{emp}, psf	1.1	
Ultimate Load Factor, g's	5.7 assumed	
Surface Areas, ft^2		
Wing, S	47.4	
Horiz. Tail, S_h	10.5	
Vert. Tail, S_v	5.0	
Empenn. Area, S_{emp}	15.5	

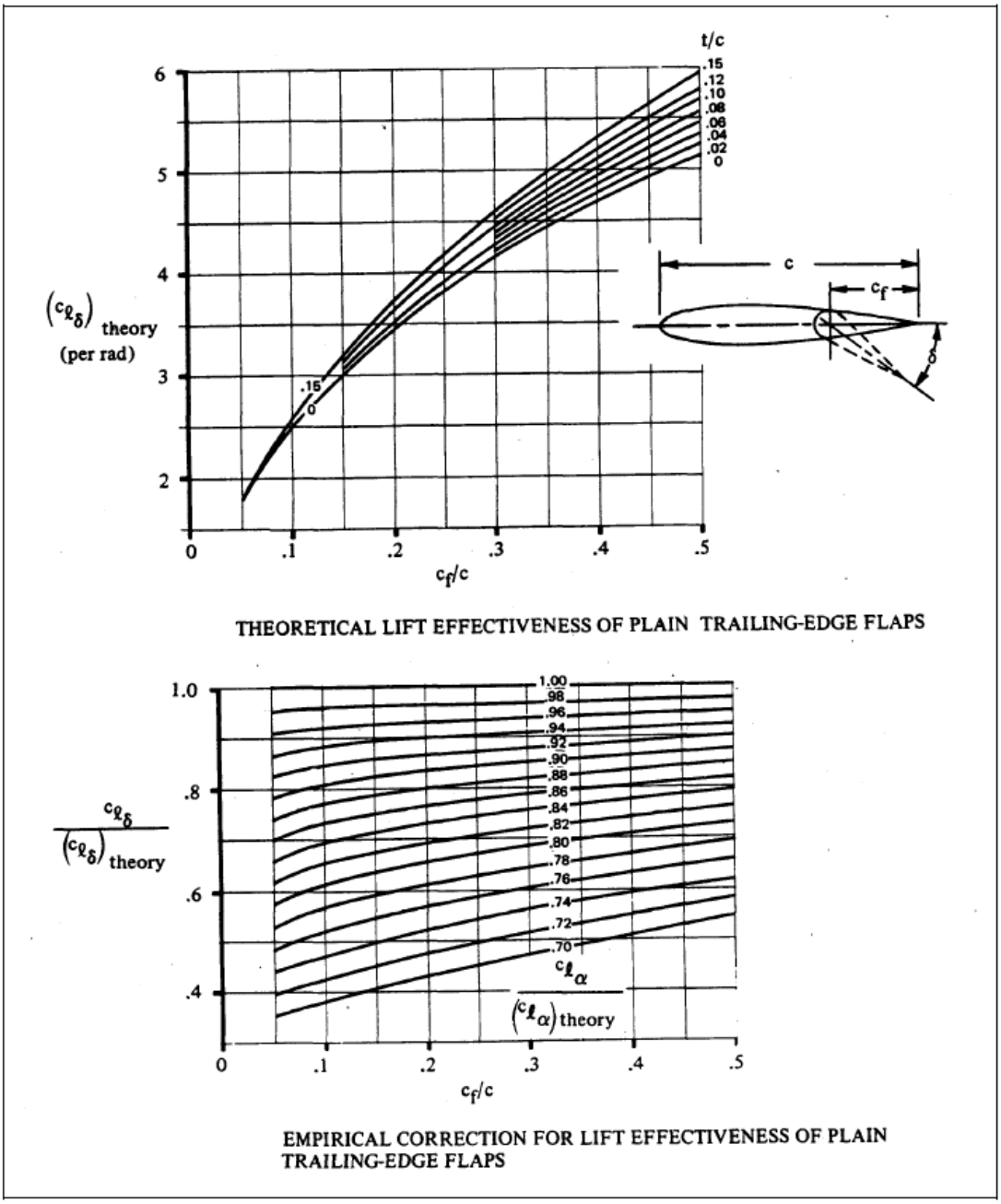

Figure A.1 Increase in lift (Scholz 2015, Sec. 11.4, Fig. 11.15)

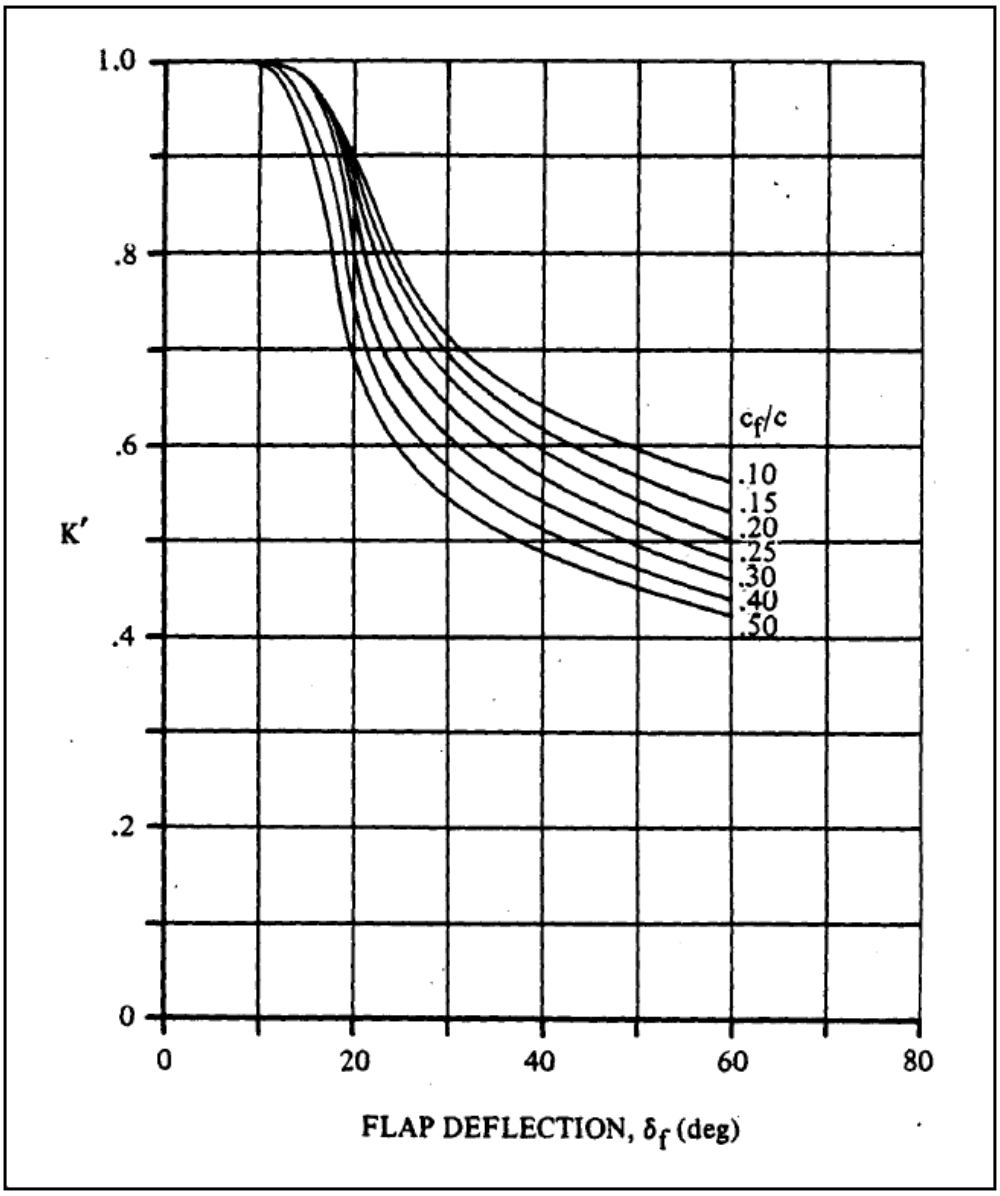

Figure A.2 Empirical correction for nonlinear effect at bigger flap angles (Scholz 2015, Sec. 11.4, Fig. 11.17)

Appendix B – Trade-off Study Table

PAGE INTENTIONALLY LEFT BLANK

Table B.1a Drone models

Name	Distributor	max. Speed [km/h]	Range [km]	Endurance [min]	Service Ceiling [m] AMSL	max. Payload [kg]	MTOW [kg]	W_E [kg]	Engine	Fuel	Power [W]	Horizontal propulsion	Launch	Recovery	Dimensions [m] x [m]	Sensors
S1-V300	UAVOS	220	4020	1680	6000	300				petrol	193882	single-prop	Airstrip	Airstrip	18,7 x 8,7	EO/IR, SAR, ISR
RAYBIRD 3	Skyeton	140	2500	1680	4500	5	21	12		petrol		single-prop	Catapult	Parachute, Airbag	2,96	Early fire detection, EO, Radar, Multi
The Black Swan	Dronamics	200	2500	750	6096	350				petrol		single-prop	Airstrip	Airstrip	16 x 8 x 4	N/A
ALBATROSS 2.2	UAVOS	205	2255	660	7200	250	550	300	ROTAX 912IS	petrol	68000		paved RWY	paved RWY	14,97 x 6,5	
Primoco UAV One 150	Primoco UAV SE	150	2000	900	3300	30	150	90	Primoco Engine 340	petrol	18642	single-prop	Airstrip	Airstrip	4,85 x 3,65 x 1,25	EO, MWIR, Laser Range-finder, Li-DAR
Flexrotor	Volatus Aero-space	140	2000	1411	6500	7,7	25	14		petrol		single-prop	VTOL	VTOL	3,0 x 2,0 x 2,2	
ORYX	CAT UAV	130	1872	1560		7,5	22	14,5	GF40U-FI	petrol	2000	single-prop	Airstrip	Airstrip	3,0 x 2,27 x 0,7	
XV-L ERC	Plymouth Rock Technol-ogies Inc.	169	1013	540	4572	20				petrol		single-prop	VTOL	VTOL	5,0 x 3,4	
PD-2 Fixed-Wing UAS (with chassis)	UKRSPECSYST EMS	140	1000	600	4700	19				petrol		single-prop	Airstrip	Airstrip	5,0 x 2,85	EO/IR/LRF, SAR Radar, LiDAR, Radio Repeater
SITARIA-E	UAVOS	140	900	720	5000	10	38	27		petrol		single-prop	Airstrip	Airstrip	4,3 x 2,8	
FDG50F	Fly Dragon Drone Tech.	130	850	420	4000	15				petrol		single-prop	VTOL	VTOL	4,8 x 2,58	
Vedette M	Volatus Aero-space		800	1440		18,14				petrol		single-prop	Catapult	Belly		
XV-L	Plymouth Rock Technol-ogies Inc.	169	788	420	3048	25				petrol		single-prop	VTOL	VTOL	5,0 x 3,4	
S360Mk.II	Hanseatic Aviation Solu-tions	140	700	420		5	30			electric		single-prop	Airstrip	Airstrip	3,6	Universal, swappable
Heavy load VTOL	Fly Dragon Drone Tech.	180	648	360	5000	55	100			petrol		single-prop	VTOL	VTOL	5,1 x 2,905	

Table B.1b Drone models

Name	Distributor	max. Speed [km/h]	Range [km]	Endurance [min]	Service Ceiling [m] AMSL	max. Payload [kg]	MTOW [kg]	W_E [kg]	Engine	Fuel	Power [W]	Horizontal propulsion	Launch	Recovery	Dimensions [m] x [m]	Sensors
Elektra One Solar	Elektra Solar	150	560	390		110	410	180	HPD 32D	electric	32000	single-prop	Airstrip	Airstrip	14	
SkyEye Sierra	ElevonX	125	500	480		5	12,5			petrol		single-prop	Airstrip, Catapult	Airstrip, Parachute	3,0 x 1,52	
CW-25H	JOUAV	80	500	330	6000	4	31			hydro-gen		single-prop	VTOL	VTOL	4,4 x 2,1	
FD180P	Fly Dragon Drone Tech.	130	500	60	5000	40	180			petrol		single-prop	VTOL	VTOL	6,5 x 3,35	
Spirit-X	Gadfin Aero-Logistics	150	500			150				hydro-gen		single-prop	VTOL	VTOL		
FDG6E	Fly Dragon Drone Tech.	100	480	330	7000	10				electric		single-prop	VTOL	VTOL	3,8 x 2,3	
Tango	ElevonX	125	420	360		5	19			petrol		single-prop	VTOL	VTOL	3,0 x 1,9	
BOREY 20	UAVOS	108	400	300	3500	4	26	8,7		electric	2000	single-prop	Catapult	Parachute	4,37 x 0,875	
FDD50	Fly Dragon Drone Tech.	130	400	120	4000	15				petrol		single-prop	VTOL	VTOL	3,8 x 2,5	
FLY-380	Fly Dragon Drone Tech.	130	400		4000	15				petrol		single-prop	VTOL	VTOL	3,8 x 2,5	
XV-H	Plymouth Rock Technologies Inc.	112	322	240	3048	3,5				petrol		single-prop	VTOL	VTOL	2,95 x 1,4	
Pelican Cargo	Pyka	148	320	30	2438	181				electric	100000	quad-prop	Airstrip	Airstrip	11,5 x 6,8	Laser, Radar, GPS
FIXAR 025 UAV	FIXAR-AERO LLC	85	300	210	5000	10				electric		quad-prop	VTOL	VTOL	2,8	Multi, LiDAR
SKYLANE-350	Sky-Drones Technologies LTD	100,8	300	150	3000	7				electric		single-prop	VTOL	VTOL	3,5 x 1,88	
Albatross	Applied Aeronautics	129	250	240		4,4				electric		single-prop	Airstrip	Airstrip	3,0 x 0,74	
XV	Plymouth Rock Technologies Inc.	112	241	180	3048	2,5				electric		single-prop	VTOL	VTOL	2,95 x 1,4	
SkyEye Delta	ElevonX	100	200	210		2				electric		single-prop	Catapult	Belly, Parachute	2,29 x 0,99	
Penguin C	EDGE Autonomy	111,12	180	1200	5000		25			petrol		single-prop	Catapult	Parachute, Airbag	3,3	EO/IR

Table B.1c Drone models

Name	Distributor	max. Speed [km/h]	Range [km]	Endurance [min]	Service Ceiling [m] AMSL	max. Payload [kg]	MTOW [kg]	W_E [kg]	Engine	Fuel	Power [W]	Horizontal propulsion	Launch	Recovery	Dimensions [m] x [m]	Sensors
Penguin C Mk 2.5 VTOL	EDGE Autonomy	120,38	180	720	5000					petrol, electric		single-prop	VTOL	VTOL	4,12	EO/IR
Elektra VTOL	Elektra Solar	80	180	180		2				electric	165	twin-prop	VTOL	VTOL	2,5	
VXE30	EDGE Autonomy	92,6	160	480	4572					SOFC, propane		single-prop	VTOL	VTOL	4,9	EO/IR
ATLAS-V (fuel)	Airborne Drones	100	150	900	3000	3				petrol		single-prop	VTOL	VTOL	3,2	EO/IR
QP530	AheadX	75	150	180	4000					electric		single-prop	VTOL	VTOL	3,0 x 1,55	EO/IR
QP532	AheadX	90	150	180	5500					electric		single-prop	VTOL	VTOL	3,2 x 1,74	EO/IR
Long-Range Surveillance Drone	Draganfly	108	130	120	3048	1,5				electric		single-prop	VTOL	VTOL	3,5 x 1,86	EO/IR
UAS100	Thales Group	150	100	300	3048	10				petrol, electric		tri-prop	Airstrip	Airstrip	5,4 X 3,3	
ATLAS-V (electric)	Airborne Drones	100	100	180	3000	3				electric	4000	single-prop	VTOL	VTOL	3,2	EO/IR
Sentaero 5	Censys Technologies	64,37	88,5	90						electric		twin-prop	VTOL	VTOL		Universal, swappable
Pelican Spray	Pyka	148	9,5	30		317				electric	75000	tri-prop	Airstrip	Airstrip	11,5 x 6,0	LiDAR, Laser, Radar, GPS
M2	Rapidflight			2160		27,2				petrol		single-prop				EO/IR, SAR Radar, SIGINT, comm relay
AXR	Tekever	300		1440		150				petrol		twin-prop				
Endurance 900	EOS Technologies			1440	5000	20				electric, solar		twin-prop	Airstrip	Airstrip	9 x 3,5	
ThunderB	BlueBird Aero Systems	130		1440	4876,8	4				petrol		single-prop	Catapult	Parachute	4,0 x 1,9	EO/IR, LiDAR
AR5	Tekever	100		1200		50				petrol		twin-prop	Airstrip	Airstrip	7,3 x 4,0	EO/IR, AIS and EPIRB, Maritime Radar, Synthetic Aperture Radar

Table B.1d Drone models

Name	Distributor	max. Speed [km/h]	Range [km]	Endurance [min]	Service Ceiling [m] AMSL	max. Payload [kg]	MTOW [kg]	W_E [kg]	Engine	Fuel	Power [W]	Horizontal propulsion	Launch	Recovery	Dimensions [m] x [m]	Sensors
AR3	Tekever	90		960	3600	4				petrol		single-prop	Cata-pult, VTOL	Parachute, Net, Belly, Water, VTOL	3,5 x 1,9	EO, LWIR, Laser illumi-nators, comm relay
AR3 NET RAY	Tekever	120		600		8				electric		single-prop	Catapult	Parachute, Net	3,2 x 1,4	EO, LWIR, Laser illumi-nators, comm relay, biological and chemi-cal analys-ers, Mari-time Radar, AIS, LiDAR
Strix 400	EOS Techno-logies	120		600	5000	2,5				electric , solar		single-prop	Hand	Belly	4,25 x 1,85	EO, IR, Laser Rangefinder
CW-80E	JOUAV	100		480	5000	20				electric , petrol		single-prop	VTOL	VTOL	5,0 x 3,1	
FLY-330	Fly Dragon Drone Tech.	120		480	4500	10				petrol		single-prop	VTOL	VTOL	3,3 x 2,1	
CW-30E	JOUAV	90		480	6000	8				electric , petrol		single-prop	VTOL	VTOL	4,4 x 2,4	
PD-1 Fixed-Wing UAV	UKRSPECSYST EMS	140		900	3000	10	40	22		petrol		single-prop	Airstrip, Catapult	Airstrip, Parachute	4,7 x 2,5	EO/IR, SAR Radar, Radio Repeater
CW-25	JOUAV	100		360	7000	6				electric , patrol		single-prop	VTOL	VTOL	4,0 x 2,1	
Vyom-12 Fixed Wing Uav	TechnoSys Embedded Systems (P) Ltd	120		240	4500	25				petrol		single-prop	Airstrip	Airstrip	6,0 x 3,4	
CW-25E	JOUAV	72		240	6000	6				electric		single-prop	VTOL	VTOL	4,35 x 2,08	
Vedette E	Volatus Aero-space			180		18,14				electric		single-prop	Catapult	Belly		
CW-15	JOUAV	61		180	6500	3				electric		single-prop	VTOL	VTOL	3,54 x 2,06	
SKIRON-X	Aurora Flight Sciences	92,6		180		1,45				electric		single-prop	VTOL	VTOL	5,0 x 2,2	EO/IR

Table B.1e Drone models

Name	Distributor	max. Speed [km/h]	Range [km]	Endurance [min]	Service Ceiling [m] AMSL	max. Payload [kg]	MTOW [kg]	W_E [kg]	Engine	Fuel	Power [W]	Horizontal propulsion	Launch	Recovery	Dimensions [m] x [m]	Sensors
FLY-350	Fly Dragon Drone Tech.	110		120		6			5322 KV430	electric	2400	single-prop	VTOL	VTOL	3,5 x 1,61	
S180Mk.II	Hanseatic Aviation Solutions			35		1				electric		single-prop			1,8	Universal, swappable
Elektra Eagle	Elektra Solar	120			20000	100	600	360	HPD 32D	electric	32000	single-prop	Airstrip	Airstrip	37,8	
AL-150	Aeroland UAV Inc.	140		960	5000	40	150	50		petrol	23900	single-prop	Airstrip	Airstrip	8,0 x 3,5	
Smart Eye 1	ADCOM Systems	150		120	3000	40	100	50		petrol	25354	twin-prop	Airstrip	Airstrip	4,4 x 3,3	
ScanEagle	Insitu	148		1200	5950	5	26,5	18		petrol	1120	single-prop	Airstrip	Airstrip	3,11 x 1,71	
RQ-21 Blackjack	Insitu	170		960	5900		61	37		petrol	6000	single-prop	Airstrip	Airstrip	4,9 x 2,5	

Appendix C – Database of Motor Gliders

Table C.1a Database of motor glider

	Model	**Wingspan [m]**	**AR [-]**	**S_W [m^2]**	**m_E [kg]**	**m_{TO} [kg]**	**m/S [kg/m^2]**	**m_E/m_{TO} [-]**
1	Pietruszka Axel	12,2		10,9	78	185		0,4216
2	Ruppert Electeryx	13,6		12,8	90	191		0,4712
3	Straton D-8	12	18	10,3	113	213	20,7	0,5305
4	Mini Straton D-7	12		9,8	113,4	213,2		0,5319
5	Aerola Alatus M	13,1	13,3	13,6	115	235	15,2	0,4894
6	Altinger TA-31 Ñahatí	13	17,33	9,75	140	240	24,6	0,5833
7	Piuma Evoluzione	11,8	13	10,6	150	240	22,6	0,6250
8	Piuma Tourer	10,4	11,7	9,2	158,8	250	27	0,6352
9	US Aviation Cumulus	13,11		13,1	145	254		0,5709
10	Alisport Silent Club A302efi	12	14	10,3	175	290		0,6034
11	Air Energy AE-1 Silent	12	14	10,3	195	300		0,6500
12	Alisport Silent 2 A302efi	13	19,2	8,8	175	300	34	0,5833
13	Barel Graal	15	22,5	10	200	300		0,6667
14	Pastel MN 600 K	10			200	300		0,6667
15	Alisport Silent 2 Electro	13,2	20	8,9	205	310	34	0,6613
16	Alisport Silent 2 Targa A302	13,3	20	8,9	190	315	34	0,6032
17	EMG-6	11	8	16,1	159	340		0,4676
18	ProFe D-10 Tukan	14,7	14,7	14,7	220	420	28,6	0,5238
19	Piuma Twin Evoluzione	13		12,2	270	440		0,6136
20	Pipistrel Taurus	15,2	18,6	12,26	295	473	12,33	0,6237
21	Schempp-Hirth Discus 2C FES	18	28,5	11,36	340	565	49,6	0,6018
22	HpH 304ES Shark	18	27,4	11,8	365	600	37	0,6083
23	LAK-17B FES	18	31,4	10,32	295	600	58,13	0,4917

Table C.1b Database of motor glider

	Model	Wingspan [m]	AR [-]	S_W [m^2]	m_E [kg]	m_{TO} [kg]	m/S [kg/m^2]	m_E/m_{TO} [-]
24	Scheibe Falke	18,2	13,8		435	650		0,6692
25	Schleicher ASW 22BE	26,6	42,3	16,7	510	750		0,6800
26	Schleicher ASH 25 Mi	25,6	39,8	16,5	478	750		0,6373
27	Schleicher ASG-32 El	20	25,5	15,7	585	850	41,7	0,6882
28	Leichtwerk eta	30,9	51,33	18,6	650	850	45,7	0,7647
29	Lange Antares 23E	23	38,3	14,75	510	850		0,6000
30	Binder EB28	28	46,7	16,8	570	850		0,6706
31	Binder EB29	29,3	51	16,8	570	850		0,6706